Dynamic bimodality of curli expression in planktonic cultures of *Escherichia coli* is stabilized by cyclic-di-GMP regulation

Olga Lamprecht[1†], Maryia Ratnikava[1], Paulina Jacek[1], Eugen Kaganovitch[1], Nina Buettner[1], Kirstin Fritz[1], Robin Köhler[1], Julian Pietsch[1], and Victor Sourjik[1*]

[1]Max Planck Institute for Terrestrial Microbiology and Center for Synthetic Microbiology (SYNMIKRO), Karl-von-Frisch Strasse 16, 35043 Marburg, Germany

[†]Present address: Eawag: Swiss Federal Institute of Aquatic Science and Technology, Dübendorf, Switzerland

*Corresponding author: Victor Sourjik, victor.sourjik@synmikro.mpi-marburg.mpg.de

Abstract

Curli amyloid fibers are major constituent of the extracellular biofilm matrix formed by bacteria of the Enterobacteriaceae family. Within *Escherichia coli* biofilms, curli gene expression is limited to a subpopulation of bacteria, leading to heterogeneity of extracellular matrix synthesis. Here we show that bimodal activation of curli expression also occurs in well-mixed planktonic cultures of *E. coli*, resulting in stochastic differentiation into distinct subpopulations of curli-positive and curli-negative cells at the entry into the stationary phase of growth. Monitoring curli activation in individual *E. coli* cells growing in a microfluidic device revealed that the curli-positive state is only metastable and it can spontaneously revert during continuous growth in a conditioned medium. The regulation by c-di-GMP is not required for curli gene activation or for differentiation of *E. coli* in subpopulations of curli-producing and curli-negative cells. Instead, we observe that c-di-GMP modulates the probability and dynamics of stochastic curli activation and enhances stability of the curli-positive state.

Keywords: Gene expression, bacteria, biofilm, bistability, differentiation, amyloid fibers

Introduction

Curli amyloid fibers are the key component of the extracellular matrix produced during biofilm formation by *Escherichia coli*, *Salmonella enterica*, and other Enterobacteriaceae [1-9]. In *E. coli* and *S. enterica* serovar Typhimurium, curli genes are organized in two divergently transcribed *csgBAC* and *csgDEFG* operons that share a common intergenic regulatory region [10]. Expression of these operons is under regulation of the stationary phase sigma factor σ^S (RpoS) and thus becomes activated during the entry into the stationary phase of growth [4, 11-14]. This activation is achieved by the σ^S-dependent induction of the transcriptional regulator CsgD, which then controls the expression of the *csgBAC* operon that encodes the major curli subunit CsgA along with the curli nucleator CsgB and the chaperone CsgC [7, 8, 15]. In turn, *csgD* expression in *E. coli* and *S.* Typhimurium is either directly or indirectly regulated by multiple cellular factors that mediate responses to diverse environmental changes, including both global and specific transcriptional regulators, small regulatory RNAs and second messengers (reviewed in [16-19]).

One of the key regulators of *csgD* is the transcription factor MlrA [13, 14, 20, 21]. The activity of MlrA depends on cellular levels of bacterial second messenger bis-(3'-5')-cyclic dimeric guanosine monophosphate (c-di-GMP), and in *E. coli* this control is known to be mediated by a pair of the interacting diguanylate cyclase (DGC) and phosphodiestherase (PDE) enzymes, DgcM and PdeR, that form a ternary complex with MlrA [12, 14, 22]. MlrA is kept inactive by binding PdeR, and this interaction is relieved when the latter becomes active as a PDE thus acting as the trigger enzyme [22, 23]. This inhibition is counteracted by DgcM that locally produces c-di-GMP to engage PdeR, as well as by the global pool of c-di-GMP. Besides its enzymatic activity, DgcM might also activate MlrA through direct protein interaction. Another DGC-PDH pair, DgcE and PdeH, provides global regulatory input into the local DgcM-PdeR-MlrA regulation [12, 24].

Previous studies of *E. coli* macrocolony biofilms formed on agar plates showed that curli expression occurs in the upper layer of the colony, but even in this layer its expression remained heterogeneous [25-27], indicating an interplay between global regulation of curli gene expression by microenvironmental gradients within biofilms and its inherent stochasticity. Differentiation of *E. coli* into distinct subpopulations of cells either expressing or not expressing curli was also observed in submerged biofilms formed in liquid cultures, whereby curli expression was associated with cellular aggregation [28]. Furthermore, bi- or multimodality of *csgD* reporter activity was also observed in the early stationary phase among planktonic cells in *S.* Typhimurium [29, 30] and *E. coli* [27]. Given established c-di-GMP-dependent regulation of CsgD activity, it was proposed that bistable curli expression originates from a toggle switch created by mutual inhibition between DgcM and PdeR, which could act as a bistable switch [27, 31].

68 In this study we demonstrate that stochastic differentiation of *E. coli csgBAC* operon
69 expression into distinct subpopulations of curli-positive and -negative cells occurs during the
70 entry into the stationary phase in a well-stirred planktonic culture, and thus in absence of any
71 environmental gradients. Similar stochastic and reversible differentiation could be observed
72 among cells growing in conditioned medium in the microfluidic channel. The upstream
73 regulation by c-di-GMP is not required to establish the bimodality of curli expression, but it
74 determines the fraction of curli-positive cells and enhances the stability of curli activation.
75

76 ## Materials and methods

77 ### Bacterial strains and plasmids

78 All strains and plasmids used in this study are listed in Table S1. Derivative of *E. coli* W3110
79 [26] that was engineered to encode a chromosomal transcriptional sfGFP reporter downstream
80 of the *csgA* gene [28] (VS1146) was used here as the wildtype strain. Gene deletions were
81 obtained with the help of P1 phage transduction using strains of the Keio collection [32] as
82 donors, and kanamycin resistance cassette was removed using FLP recombinase [33]. For
83 expression, *dgcE* and *pdeH* genes were cloned into pTrc99A vector [34].
84

85 ### Growth conditions for planktonic cultures

86 Planktonic *E. coli* cultures were grown in tryptone broth (TB) medium (10 g tryptone, 5 g NaCl
87 per liter), supplemented with antibiotics where necessary. Overnight cultures grown at 30°C
88 were diluted 1:100, unless indicated otherwise, in 5-10 ml of fresh TB and grown at 30°C at
89 200 rpm in 100 ml flasks in a rotary shaker until indicated OD_{600} or overnight (18-25 h; OD_{600}
90 ~ 1.3-1.8). Alternatively, cultures were grown in 96-well plates with linear shaking in a plate
91 reader, with 200 µl culture per well. Where indicated, bacterial cultures were supplemented
92 with either 1 mM L-serine (after 6 h of growth) or 0.1–10 mg/l DL-serine hydroxamate at
93 inoculation.
94

95 ### Growth and quantification of submerged biofilms

96 Submerged biofilms were grown and quantified as described previously [28], with minor
97 modifications. Overnight bacterial cultures grown in TB were diluted 1:100 in fresh TB medium
98 and grown at 200 rpm and 30°C in a rotary shaker to OD_{600} of 0.5. These cultures were then
99 diluted in fresh TB medium to a final OD_{600} of 0.05, and 300 µl was loaded onto a 96-well plate
100 (Corning Costar, flat bottom; Sigma-Aldrich, Germany) and incubated without shaking at 30°C
101 for 46 h.
102 For quantification of biofilm formation, the non-attached cells were removed and the wells were
103 washed once with phosphate-buffered saline (PBS; 8 g NaCl, 0.2 g KCl, 1.44 g Na_2HPO_4, 0.24
104 g KH_2PO_4). Attached cells were fixed for 20 min with 300 µl of 96% ethanol, allowed to dry for

105 40 min, and stained with 300 µl of 0.1% crystal violet (CV) solution for 15 min at room
106 temperature. The wells were subsequently washed twice with 1x PBS, incubated with 300 µl
107 of 96% ethanol for 35 min and the CV adsorption was measured at OD_{595} using INFINITE M
108 $NANO^+$ plate reader (Tecan Group Ltd., Switzerland). These CV values were normalized to
109 the OD_{600} values of the respective biofilm cultures.
110
111 **Macrocolony biofilm assay**
112 Macrocolony biofilms were grown as described previously [26]. Briefly, 5 µl of the overnight
113 liquid culture grown at 37°C in lysogeny broth (LB) medium (10 g tryptone, 10 g NaCl, and 5 g
114 yeast extract per liter) was spotted on salt-free LB agar plates supplemented with Congo red
115 (40 µg/ml). Plates were incubated for 8 days at 28°C.
116
117 **Fluorescence measurements**
118 Measurements of GFP expression in an INFINITE M1000 PRO plater reader (Tecan Group
119 Ltd., Switzerland) were done using fluorescence excitation at 483 nm and emission at 535 nm.
120 Relative fluorescence was calculated by normalizing to corresponding OD_{600} values of the
121 culture.
122 For fluorescence measurements using flow cytometry, aliquots of 40-300 µl of liquid bacterial
123 cultures were mixed with 2 ml of tethering buffer (10 mM KH_2PO_4, 10 mM K_2HPO_4, 0.1 mM
124 EDTA, 1 µM L-methionine, 10 mM lactic acid, pH 7.0). Macrocolonies were collected from the
125 plate, resuspended in 10 ml of tethering buffer and then aliquots of 40 µl were mixed with 2 ml
126 of fresh tethering buffer. Samples were vigorously vortexed and then immediately subjected to
127 flow cytometric analysis using BD LSRFortessa Sorp cell analyzer (BD Biosciences, Germany)
128 using 488-nm laser. In each experimental run, 50,000 individual cells were analyzed. Absence
129 of cell aggregation was confirmed by using forward scatter (FSC) and side scatter (SSC)
130 parameters. Data were analyzed using FlowJo software version v10.7.1 (FlowJo LLC,
131 Ashland, OR, US), applying a software-defined background fluorescence subtraction.
132
133 **Microfluidics**
134 Conditioned medium was prepared by cultivating wildtype *E. coli* in TB in a rotary shaker at
135 30°C for 20 h, after which the cell suspension was centrifuged at 4000 rpm for 10 min, medium
136 was filter-sterilized and stored at 4°C. Mother machine [35] microfluidics device was designed,
137 fabricated and operated as described in Supporting protocols. *E. coli* cells from the overnight
138 culture in TB were loaded into the mother machine growth sites by manual infusion of the cell
139 suspension through one of the two inlets using a 1-ml syringe. Cells were first allowed to grow
140 at 30 °C for 4 h in fresh TB, then switched to the conditioned TB and cultivated for up to 26 h.
141 Phase contrast and GFP fluorescence images were acquired using a Nikon Eclipse Ti-E

142 inverted microscope with a time interval of 10 min. Details of image analysis are described in
143 Supporting protocols.
144
145 ## Results
146 **Bimodal curli expression is induced in planktonic culture**
147 In order to characterize curli expression in planktonic culture of *E. coli*, we followed the
148 induction of chromosomal transcriptional reporter of *csgBAC* operon, where the gene encoding
149 for green fluorescent protein (GFP) was cloned with a strong ribosome binding site as a part
150 of the same polycistronic RNA downstream of *csgA* [28]. In our previous study of submerged
151 *E. coli* biofilms, this reporter showed bimodal expression both in the surface-attached biofilm
152 and in the pellicle at the liquid-air interface [28]. When *E. coli* culture was grown at 30°C in
153 tryptone broth (TB) liquid medium, this reporter became induced during transition to the
154 stationary phase (Figure 1A), which is consistent with previous reports [12, 14]. The observed
155 induction of curli expression occurred at similar density in the cultures with different initial
156 inoculum size. In both cases the onset of induction apparently coincided with the reduction of
157 the growth rate, which likely occurs due to depletion of amino acids in the medium and
158 induction of the stringent response [36, 37], consistent with proposed role of stringent response
159 in the regulatory cascade leading to curli gene expression [18, 23]. In agreement with that,
160 curli expression was strongly reduced when *E. coli* culture was grown in a concentrated TB
161 medium (Figure S1A) or when TB medium was supplemented with serine (Figure S2A).
162 Moreover, the induction of curli reporter was strongly enhanced by addition of serine
163 hydroxamate (SHX), which is known to mimic amino acid starvation and induce stringent
164 response [38] (Figure S2A).
165 In order to investigate whether curli expression was uniform or heterogeneous across
166 planktonic *E. coli* population, we next measured curli reporter activity in individual cells using
167 flow cytometry. The reporter was induced only in a fraction of cells, and this bimodality of curli
168 expression became increasingly more pronounced at later stages of culture growth, reaching
169 its maximum in the overnight culture (Figure 1B). Thus, the bimodal induction of curli gene
170 expression is observed not only in biofilms but also in a well-mixed planktonic culture. While
171 curli activation was more pronounced in a cell culture growing in an orbital shaker (Figure 1B),
172 bimodality was also observed during culture growth in the plate reader (Figure S1B). Notably,
173 stimulation of curli expression by SHX or its suppression by additional nutrients affected the
174 fraction of positive cells rather than their expression levels (Figure S1B and Figure S2B).
175
176 **Bimodality of curli expression does not require regulation by c-di-GMP**
177 Subsequently, we investigated dependence of curli expression in planktonic culture on the
178 upstream regulation by c-di-GMP (Figure 2A). As expected, no activation of curli reporter was

179 observed in the absence of MlrA (Figure 2B). Curli expression was also affected by the lack of
180 enzymes that control MlrA activity at the global (DgcE and PdeH) or local (DgcM and PdeR)
181 level of c-di-GMP regulation (Figure 2C). Consistently with their established regulatory roles,
182 deletions of cyclase genes *dgcE* and *dgcM* resulted in nearly all cells being curli-negative,
183 whereas deletions of diesterase genes *pdeH* and *pdeR* led to activation of curli expression in
184 the majority of cells within the planktonic population. Notably, in all cases a small fraction of
185 positive (for cyclase knockouts) or negative (for esterase knockouts) cells could be detected,
186 indicating that neither of these knockouts entirely eliminates the bimodality of curli expression.
187 This conclusion could be further confirmed by combined deletions of cyclase and diesterase
188 genes. Removal of the entire global level of c-di-GMP regulation in Δ*pdeH* Δ*dgcE* strain led to
189 a bimodal pattern of curli activation (Figure 2D) that was similar to that observed in the wildtype
190 cells. Even more surprisingly, the distribution of curli expression remained bimodal upon
191 removal of the local level of c-di-GMP regulation in Δ*pdeR* Δ*dgcM* strain, although the fraction
192 of curli-positive cells was reduced and heterogeneity of their expression levels increased in
193 this background. The bimodality of curli expression was also retained in the quadruple
194 knockout strain lacking all four cyclase and diesterase genes (Figure 2E). Thus, whereas both
195 global and local c-di-GMP-dependent regulation of MlrA activity clearly affect the fraction of
196 curli-positive cells, they are apparently not required to activate curli expression or to establish
197 its bimodality in the planktonic cell population.
198 *Vibrio cholerae* transcriptional regulator VpsT, a close homologue of CsgD, has been shown
199 to be directly regulated by binding to c-di-GMP [39]. Furthermore, in *S.* Typhimurium c-di-GMP
200 was proposed to regulate *csgD* expression not only at transcriptional but also at a
201 posttranscriptional level [40]. We thus aimed to verify that *E. coli* curli gene expression was no
202 longer sensitive to the global cellular level of c-di-GMP in the absence of the local PdeR/DgcM
203 regulatory module. Indeed, whereas the overexpression of c-di-GMP cyclase DgcE or
204 phosphodiesterase PdeH had strong impacts on the fraction of curli-positive cells in the
205 wildtype, the quadruple mutant was insensitive to such overexpression (Figure S3), confirming
206 that in this background the expression of the *csgBAC* reporter is no longer affected by the
207 global pool of c-di-GMP.
208
209 **Curli activation shows higher variability in absence of c-di-GMP regulation**
210 We next explored how the fraction of curli-positive cells in the population depends on the
211 conditions of culture growth, with and without regulation by c-di-GMP. As mentioned above,
212 even in the wildtype strain the fraction of curli-positive cells was smaller in cultures grown in
213 multi-well plates (Figure S1B) compared to the incubation in the flask in an orbital shaker
214 (Figure 1B). However, this reduction in the number of curli-positive cells was much more
215 pronounced for Δ*pdeR* Δ*dgcM* or Δ*pdeH* Δ*dgcE* Δ*pdeR* Δ*dgcM* strains, where only a small

216 fraction of cells became positive under these growth conditions (Figure 3A,B and Figure S4).
217 Also individual *dgc* and *pdh* gene knockout strains showed reduced activation of curli reporter
218 (Figure S4). Of note, another difference with the flask culture was that the low-fluorescence
219 peak of the wildtype culture was not fully negative but apparently contained a large fraction of
220 cells with incompletely activated curli reporter, which could also be seen in Δ*pdeH* or Δ*pdeR*
221 knockouts but not in the Δ*pdeH* Δ*dgcE* Δ*pdeR* Δ*dgcM,* Δ*pdeR* Δ*dgcM* or Δ*pdeH* Δ*dgcE* strains
222 (Figure 3B and Figure S4). Similar results were obtained even upon prolonged incubation in
223 the plate reader (Figure S5), confirming that the observed difference with the overnight flask
224 culture was not because of the different growth stage.
225 We further tested reporter activation under growth conditions that favour biofilm formation.
226 During formation of static submerged biofilms in multi-well plates where cultures are grown
227 without shaking, the overall curli activation in the populations of Δ*pdeH* Δ*dgcE*, Δ*pdeR* Δ*dgcM*
228 or Δ*pdeH* Δ*dgcE* Δ*pdeR* Δ*dgcM* cells (Figure 3C) as well as in the individual knockout strains
229 (Figure S6A) was comparable to that in the culture grown in the orbital shaker (Figure 2B-E).
230 Curli gene activation in individual mutant strains correlated well with the levels of submerged
231 biofilm formation (Figure S6B), although the lack of regulation by c-di-GMP resulted in stronger
232 reduction of the biofilm biomass, consistent with other roles of c-di-GMP in biofilm formation
233 besides curli regulation.
234 We also grew all strains in the form of macrocolony biofilms on an agar plate [26]. Interestingly,
235 here the extent of reporter activation in the Δ*pdeR* Δ*dgcM* and Δ*pdeH* Δ*dgcE* Δ*pdeR* Δ*dgcM*
236 strains was much higher and comparable to that of the wildtype (Figure 3D) and even individual
237 Δ*dgcE* and Δ*dgcM* knockouts showed high fraction of curli-positive cells (Figure S7A),
238 consistent with their stronger Congo red staining compared to the Δ*mlrA* negative control
239 (Figure S7B). Summarily, these results confirm that the regulation by c-di-GMP is not required
240 for (bimodal) curli activation, but also suggest that in absence of this control the fraction of
241 culri-positive cells is more sensitive to growth conditions.
242
243 **Curli activation is a stochastic and reversible process stabilized by c-di-GMP**
244 In order to investigate the dynamics of curli activation, and the effects of c-di-GMP regulation,
245 at the single-cell level, we utilized “mother machine”, a microfluidic device where growth of
246 individual bacterial cell lineages could be followed in a highly parallelized manner over multiple
247 generations [35] (Figure 4, Figure S8 and Supporting protocols). To activate curli expression
248 in continuously growing single cells by mimicking nutrient depletion, *E. coli* wildtype or Δ*pdeH*
249 Δ*dgcE* Δ*pdeR* Δ*dgcM* cells were first loaded into the mother machine from the overnight
250 culture, allowed to grow in fresh TB medium for several generations and then shifted to the TB
251 medium that was pre-conditioned by growing the batch culture (see Materials and Methods
252 and Supporting protocols). For both strains, a fraction of curli-positive cells was observed at

253 the beginning of the experiment since cells originated from the overnight culture, but all cells
254 turned off curli expression after resuming exponential growth in the fresh medium (Figure 4A,B,
255 Figure S9, Figure S10, Figure S11, Movie S1 and Movie S2). Following shift to the conditioned
256 medium, cell growth rate was strongly reduced (Figure 4A,C,E and Figure S9A) to
257 approximately the same low growth rate for both strains. After several generations of slow
258 growth in the conditioned medium, individual cells of both strains activated curli expression,
259 while other cells remained in the curli-off state (Figure 4A,C and Figure S11). Importantly, we
260 observed that after several generations in the curli-on state, individuals cells of both strains
261 turned curli expression off again during continuous growth in the conditioned medium (Figure
262 4B,D and Figure S10), and in some cases there was even a second activation event.
263 Despite these overall similarities, the dynamics of curli reporter activation showed several
264 differences between the wildtype and the Δ*pdeH* Δ*dgcE* Δ*pdeR* Δ*dgcM* strain. Most clearly, the
265 rate of curli activation in individual cells was apparently higher in absence of the c-di-GMP
266 regulation (Figure 4B,D,F, Figure S10, Figure S12 and Figure S13). Additionally, the induction
267 showed greater intercellular heterogeneity in the Δ*pdeH* Δ*dgcE* Δ*pdeR* Δ*dgcM* strain (Figure
268 4F, Figure S10, Figure S12 and Figure S13). Thus, the control of curli expression by c-di-GMP
269 reduces the rate but increases the stability of curli induction.
270

271 **Discussion**

272 Expression of the curli biofilm matrix genes is known to be heterogeneous or even bistable in
273 communities of *E. coli* [25-28] and *S.* Typhimurium [29, 30], which might have important
274 functional consequences for the biomechanics of bacterial biofilms [27] and for stress
275 resistance and virulence of bacterial populations [29, 30]. In the well-structured microcolony
276 biofilms, differentiation into subpopulations with different levels of the curli matrix production is
277 largely deterministic and driven by gradients of nutrients and oxygen [18]. Bimodality of curli
278 expression might also emerge stochastically, in a well-mixed population or between cells within
279 the same layer of the macrocolony [27, 29, 30]. How this bimodality originates within the
280 extremely complex regulatory network of curli genes [17, 19, 23, 27] remains a matter of
281 debate. Although earlier studies in *S.* Typhimurium proposed that bistable expression of curli
282 might be a consequence of positive transcriptional feedback in *csgD* regulation [29, 30, 41],
283 the most recently proposed model attributed bistability to the properties of the c-di-GMP
284 regulatory switch formed by DgcM, PdeR and MlrA [27, 31]. Furthermore, the dynamics of curli
285 gene expression in individual cells remains unstudied.
286 Here, we investigated the bimodal expression of the major curli *csgBAC* operon at the
287 population level in the well-stirred planktonic *E. coli* culture as well as on the single-cell level
288 in the microfluidic device. Consistent with previous studies [12, 14], the induction of curli
289 expression in growing *E. coli* cell population was observed during the entry into the stationary

290 phase of growth. Curli activation was apparently dependent on depletion of the amino acids
291 from the medium, since it could be suppressed by increasing the levels of nutrients or,
292 specifically, of serine. It might thus be related to induction of the stringent response, and
293 consistently, it was enhanced by the SHX-mediated stimulation of the stringent response.
294 We further observed that activation of the *csgBAC* operon was strongly bimodal under all
295 tested conditions, even in absence of any nutrient or other gradients. Stochastic nature of this
296 activation was confirmed by incubation of *E. coli* cells in the microfluidic device, where upon a
297 shift to the conditioned medium only a fraction of the cell population turned on the curli
298 expression. Such differentiation is apparently consistent with previous observations of the
299 bimodal *csgD* expression in *S.* Typhimurium [29, 30] and in *E. coli* [27]. However, whether the
300 bimodality of the *csgBAC* expression is caused by the bimodal expression of *csgD* remains
301 clear, since the latter was reported only in the later stationary phase of the culture growth [27,
302 29, 30], whereas in our experiments the *csgBAC* reporter showed bimodality already at an
303 earlier stage.
304 In contrast to those previous interpretations of the *csgD* expression pattern as bistability, our
305 data suggest that curli activation is only transient, and therefore bimodal but not bistable. Under
306 conditions of continuous cell growth in the microfluidic device, the activation of curli expression
307 is followed by its inactivation, indicating a pulsatile activation of the curli-positive state. Pulsing
308 in expression was proposed to be common to many gene regulatory circuits [42], although only
309 few well-studied examples such as stress response and differentiation in *Bacillus subtilis* [43,
310 44] are available. Pulsatile expression has also been recently described in *E. coli* for the
311 upstream regulator of curli, RpoS [45], as well as for the flagellar regulon [46, 47] that is anti-
312 regulated with curli [28]. However, in neither of these cases did pulsing lead to apparent
313 bimodality of expression, and their relation to the observed pulses in curli expression thus
314 remains to be seen.
315 How does such stochastic pulsing of curli expression observed at the single-cell level lead to
316 the differentiation into two very distinct subpopulations in the batch planktonic culture? This
317 could be likely explained by the timing of curli activation, and by the duration of these observed
318 expression pulses: Since the curli expression is only turned-on during transition to the
319 stationary phase, individual cells can stochastically activate curli genes just before the culture
320 growth ceases. In contrast to the continuous culture, subsequent reversion to the curli-negative
321 state by inactivation and dilution by cell division is no longer possible in the stationary batch
322 culture, and these initially curli-expressing cells will thus remain positive.
323 Importantly, the regulation by c-di-GMP is not required for the bimodal curli expression in *E.*
324 *coli*, since the differentiation into distinct subpopulations still occurred when the control of CsgD
325 expression by c-di-GMP was abolished, as observed both in the planktonic cultures and in the
326 microfluidic device. The level of *csgBAC* expression in curli-positive cells was also little

327 affected by the c-di-GMP control. Nevertheless, this control is important during the
328 establishment of bimodality: Firstly, global levels of c-di-GMP determine the fraction of curli-
329 positive cells, via regulation of MlrA activity, which is respectively inhibited by PdeR when c-
330 di-GMP is low and activated by DgcM at high c-di-GMP [22, 23]. Secondly, the c-di-GMP-
331 dependent control affects the dynamics of curli gene pulsing, with the faster but more
332 heterogeneous activation of curli expression in the absence of the c-di-GMP control. Thirdly,
333 and possibly related to the previous observation, this control might also ensure that the fraction
334 of curli-positive cells is less variable dependent on the growth conditions of *E. coli* population.
335 Thus, our study reveals a novel regulatory function exhibited by the second messenger c-di-
336 GMP, in stabilizing the bimodal gene expression.
337

338 **Acknowledgements**

339 We thank Sarah Hoch, Silvia González Sierra and Gabriele Malengo for technical help and
340 advice.

341

342 **References**

343

344 1. Arnqvist A, Olsen A, Pfeifer J, Russell DG, Normark S. The Crl protein activates cryptic
345 genes for curli formation and fibronectin binding in *Escherichia coli* HB101. Mol Microbiol.
346 1992;6(17):2443-52. Epub 1992/09/01. doi: 10.1111/j.1365-2958.1992.tb01420.x. PubMed
347 PMID: 1357528.
348 2. Hufnagel DA, Depas WH, Chapman MR. The Biology of the *Escherichia coli* Extracellular
349 Matrix. Microbiol Spectr. 2015;3(3). Epub 2015/07/18. doi: 10.1128/microbiolspec.MB-0014-
350 2014. PubMed PMID: 26185090; PubMed Central PMCID: PMCPMC4507285.
351 3. Larsen P, Nielsen JL, Dueholm MS, Wetzel R, Otzen D, Nielsen PH. Amyloid adhesins
352 are abundant in natural biofilms. Environmental Microbiology. 2007. doi: 10.1111/j.1462-
353 2920.2007.01418.x.
354 4. Romling U, Bian Z, Hammar M, Sierralta WD, Normark S. Curli fibers are highly
355 conserved between *Salmonella typhimurium* and *Escherichia coli* with respect to operon
356 structure and regulation. J Bacteriol. 1998;180(3):722-31. Epub 1998/02/11. doi:
357 10.1128/JB.180.3.722-731.1998. PubMed PMID: 9457880; PubMed Central PMCID:
358 PMCPMC106944.
359 5. Vidal O, Longin R, Prigent-Combaret C, Dorel C, Hooreman M, Lejeune P. Isolation of
360 an *Escherichia coli* K-12 mutant strain able to form biofilms on inert surfaces: involvement of
361 a new ompR allele that increases curli expression. J Bacteriol. 1998;180(9):2442-9. Epub
362 1998/05/09. doi: 10.1128/JB.180.9.2442-2449.1998. PubMed PMID: 9573197; PubMed
363 Central PMCID: PMCPMC107187.
364 6. Zogaj X, Bokranz W, Nimtz M, Romling U. Production of cellulose and curli fimbriae by
365 members of the family Enterobacteriaceae isolated from the human gastrointestinal tract.
366 Infect Immun. 2003;71(7):4151-8. Epub 2003/06/24. doi: 10.1128/IAI.71.7.4151-4158.2003.
367 PubMed PMID: 12819107; PubMed Central PMCID: PMCPMC162016.

7. Tursi SA, Tukel C. Curli-Containing Enteric Biofilms Inside and Out: Matrix Composition, Immune Recognition, and Disease Implications. Microbiol Mol Biol Rev. 2018;82(4). Epub 2018/10/12. doi: 10.1128/MMBR.00028-18. PubMed PMID: 30305312; PubMed Central PMCID: PMCPMC6298610.

8. Chapman MR, Robinson LS, Pinkner JS, Roth R, Heuser J, Hammar M, et al. Role of *Escherichia coli* curli operons in directing amyloid fiber formation. Science. 2002;295(5556):851-5. Epub 2002/02/02. doi: 10.1126/science.1067484. PubMed PMID: 11823641; PubMed Central PMCID: PMCPMC2838482.

9. Dueholm MS, Albertsen M, Otzen D, Nielsen PH. Curli Functional Amyloid Systems Are Phylogenetically Widespread and Display Large Diversity in Operon and Protein Structure. PLoS ONE. 2012. doi: 10.1371/journal.pone.0051274.

10. Gerstel U, Römling U. The csgD promoter, a control unit for biofilm formation in *Salmonella typhimurium*. Research in Microbiology2003.

11. Brombacher E, Baratto A, Dorel C, Landini P. Gene expression regulation by the Curli activator CsgD protein: modulation of cellulose biosynthesis and control of negative determinants for microbial adhesion. J Bacteriol. 2006;188(6):2027-37. Epub 2006/03/04. doi: 10.1128/JB.188.6.2027-2037.2006. PubMed PMID: 16513732; PubMed Central PMCID: PMCPMC1428138.

12. Pesavento C, Becker G, Sommerfeldt N, Possling A, Tschowri N, Mehlis A, et al. Inverse regulatory coordination of motility and curli-mediated adhesion in *Escherichia coli*. Genes Dev. 2008;22(17):2434-46. Epub 2008/09/04. doi: 10.1101/gad.475808. PubMed PMID: 18765794; PubMed Central PMCID: PMCPMC2532929.

13. Romling U, Rohde M, Olsen A, Normark S, Reinkoster J. AgfD, the checkpoint of multicellular and aggregative behaviour in *Salmonella typhimurium* regulates at least two independent pathways. Mol Microbiol. 2000;36(1):10-23. Epub 2000/04/12. doi: 10.1046/j.1365-2958.2000.01822.x. PubMed PMID: 10760159.

14. Weber H, Pesavento C, Possling A, Tischendorf G, Hengge R. Cyclic-di-GMP-mediated signalling within the sigma network of *Escherichia coli*. Mol Microbiol. 2006;62(4):1014-34. Epub 2006/10/03. doi: 10.1111/j.1365-2958.2006.05440.x. PubMed PMID: 17010156.

15. Barnhart MM, Chapman MR. Curli biogenesis and function. Annu Rev Microbiol. 2006;60:131-47. Epub 2006/05/18. doi: 10.1146/annurev.micro.60.080805.142106. PubMed PMID: 16704339; PubMed Central PMCID: PMCPMC2838481.

16. Ishihama A. Prokaryotic genome regulation: Multifactor promoters, multitarget regulators and hierarchic networks. FEMS Microbiology Reviews2010.

17. Rossi E, Cimdins A, Luthje P, Brauner A, Sjoling A, Landini P, et al. "It's a gut feeling" - *Escherichia coli* biofilm formation in the gastrointestinal tract environment. Crit Rev Microbiol. 2018;44(1):1-30. Epub 2017/05/10. doi: 10.1080/1040841X.2017.1303660. PubMed PMID: 28485690.

18. Serra DO, Hengge R. Bacterial Multicellularity: The Biology of *Escherichia coli* Building Large-Scale Biofilm Communities. Annu Rev Microbiol. 2021;75:269-90. Epub 2021/08/04. doi: 10.1146/annurev-micro-031921-055801. PubMed PMID: 34343018.

19. Simm R, Ahmad I, Rhen M, Le Guyon S, Romling U. Regulation of biofilm formation in *Salmonella enterica* serovar Typhimurium. Future Microbiol. 2014;9(11):1261-82. Epub 2014/12/02. doi: 10.2217/fmb.14.88. PubMed PMID: 25437188.

20. Brown PK, Dozois CM, Nickerson CA, Zuppardo A, Terlonge J, Curtiss R. MIrA, a novel regulator of curli (AgF) and extracellular matrix synthesis by *Escherichia coli* and *Salmonella*

414 *enterica* serovar Typhimurium. Molecular Microbiology. 2001. doi: 10.1046/j.1365-
415 2958.2001.02529.x.
416 21. Ogasawara H, Yamada K, Kori A, Yamamoto K, Ishihama A. Regulation of the
417 *Escherichia coli* csgD promoter: Interplay between five transcription factors. Microbiology.
418 2010. doi: 10.1099/mic.0.039131-0.
419 22. Lindenberg S, Klauck G, Pesavento C, Klauck E, Hengge R. The EAL domain protein YciR
420 acts as a trigger enzyme in a c-di-GMP signalling cascade in *E. coli* biofilm control. EMBO J.
421 2013;32(14):2001-14. Epub 2013/05/28. doi: 10.1038/emboj.2013.120. PubMed PMID:
422 23708798; PubMed Central PMCID: PMCPMC3715855.
423 23. Hengge R. Linking bacterial growth, survival, and multicellularity - small signaling
424 molecules as triggers and drivers. Curr Opin Microbiol. 2020;55:57-66. Epub 2020/04/04. doi:
425 10.1016/j.mib.2020.02.007. PubMed PMID: 32244175.
426 24. Sarenko O, Klauck G, Wilke FM, Pfiffer V, Richter AM, Herbst S, et al. More than
427 Enzymes That Make or Break Cyclic Di-GMP-Local Signaling in the Interactome of GGDEF/EAL
428 Domain Proteins of *Escherichia coli*. mBio. 2017;8(5). Epub 2017/10/12. doi:
429 10.1128/mBio.01639-17. PubMed PMID: 29018125; PubMed Central PMCID:
430 PMCPMC5635695.
431 25. DePas WH, Hufnagel DA, Lee JS, Blanco LP, Bernstein HC, Fisher ST, et al. Iron induces
432 bimodal population development by *Escherichia coli*. Proc Natl Acad Sci U S A.
433 2013;110(7):2629-34. Epub 2013/01/30. doi: 10.1073/pnas.1218703110. PubMed PMID:
434 23359678; PubMed Central PMCID: PMCPMC3574911.
435 26. Serra DO, Richter AM, Klauck G, Mika F, Hengge R. Microanatomy at cellular resolution
436 and spatial order of physiological differentiation in a bacterial biofilm. mBio.
437 2013;4(2):e00103-13. Epub 2013/03/21. doi: 10.1128/mBio.00103-13. PubMed PMID:
438 23512962; PubMed Central PMCID: PMCPMC3604763.
439 27. Serra DO, Hengge R. A c-di-GMP-Based Switch Controls Local Heterogeneity of
440 Extracellular Matrix Synthesis which Is Crucial for Integrity and Morphogenesis of *Escherichia*
441 *coli* Macrocolony Biofilms. J Mol Biol. 2019;431(23):4775-93. Epub 2019/04/08. doi:
442 10.1016/j.jmb.2019.04.001. PubMed PMID: 30954572.
443 28. Besharova O, Suchanek VM, Hartmann R, Drescher K, Sourjik V. Diversification of gene
444 expression during formation of static submerged biofilms by *Escherichia coli*. Frontiers in
445 Microbiology. 2016. doi: 10.3389/fmicb.2016.01568.
446 29. Grantcharova N, Peters V, Monteiro C, Zakikhany K, Römling U. Bistable expression of
447 CsgD in biofilm development of *Salmonella enterica* serovar Typhimurium. Journal of
448 Bacteriology. 2010. doi: 10.1128/JB.01826-08.
449 30. MacKenzie KD, Wang Y, Shivak DJ, Wong CS, Hoffman LJ, Lam S, et al. Bistable
450 expression of CsgD in *Salmonella enterica* serovar Typhimurium connects virulence to
451 persistence. Infect Immun. 2015;83(6):2312-26. Epub 2015/04/01. doi: 10.1128/IAI.00137-15.
452 PubMed PMID: 25824832; PubMed Central PMCID: PMCPMC4432751.
453 31. Yousef KP, Streck A, Schütte C, Siebert H, Hengge R, von Kleist M. Logical-continuous
454 modelling of post-translationally regulated bistability of curli fiber expression in *Escherichia*
455 *coli*. BMC Systems Biology. 2015. doi: 10.1186/s12918-015-0183-x.
456 32. Baba T, Ara T, Hasegawa M, Takai Y, Okumura Y, Baba M, et al. Construction of
457 *Escherichia coli* K-12 in-frame, single-gene knockout mutants: the Keio collection. Mol Syst
458 Biol. 2006;2:2006 0008. Epub 2006/06/02. doi: 10.1038/msb4100050. PubMed PMID:
459 16738554; PubMed Central PMCID: PMCPMC1681482.

460 33. Cherepanov PP, Wackernagel W. Gene disruption in *Escherichia coli*: TcR and KmR
461 cassettes with the option of Flp-catalyzed excision of the antibiotic-resistance determinant.
462 Gene. 1995;158(1):9-14. Epub 1995/05/26. doi: 10.1016/0378-1119(95)00193-a. PubMed
463 PMID: 7789817.
464 34. Amann E, Ochs B, Abel K-J. Tightly regulated tac promoter vectors useful for the
465 expression of unfused and fused proteins in *Escherichia coli*. Gene. 1988;69(2):301-15. doi:
466 https://doi.org/10.1016/0378-1119(88)90440-4.
467 35. Wang P, Robert L, Pelletier J, Dang WL, Taddei F, Wright A, et al. Robust growth of
468 *Escherichia coli*. Curr Biol. 2010;20(12):1099-103. Epub 2010/06/12. doi:
469 10.1016/j.cub.2010.04.045. PubMed PMID: 20537537; PubMed Central PMCID:
470 PMCPMC2902570.
471 36. Potrykus K, Cashel M. (p)ppGpp: still magical? Annu Rev Microbiol. 2008;62:35-51.
472 Epub 2008/05/06. doi: 10.1146/annurev.micro.62.081307.162903. PubMed PMID: 18454629.
473 37. Varik V, Oliveira SRA, Hauryliuk V, Tenson T. HPLC-based quantification of bacterial
474 housekeeping nucleotides and alarmone messengers ppGpp and pppGpp. Sci Rep.
475 2017;7(1):11022. Epub 2017/09/10. doi: 10.1038/s41598-017-10988-6. PubMed PMID:
476 28887466; PubMed Central PMCID: PMCPMC5591245.
477 38. Patacq C, Chaudet N, Letisse F. Crucial Role of ppGpp in the Resilience of *Escherichia*
478 *coli* to Growth Disruption. mSphere. 2020;5(6). Epub 2020/12/29. doi:
479 10.1128/mSphere.01132-20. PubMed PMID: 33361126; PubMed Central PMCID:
480 PMCPMC7763551.
481 39. Krasteva PV, Fong JC, Shikuma NJ, Beyhan S, Navarro MV, Yildiz FH, et al. *Vibrio*
482 *cholerae* VpsT regulates matrix production and motility by directly sensing cyclic di-GMP.
483 Science. 2010;327(5967):866-8. Epub 2010/02/13. doi: 10.1126/science.1181185. PubMed
484 PMID: 20150502; PubMed Central PMCID: PMCPMC2828054.
485 40. Ahmad I, Cimdins A, Beske T, Romling U. Detailed analysis of c-di-GMP mediated
486 regulation of csgD expression in *Salmonella typhimurium*. BMC Microbiol. 2017;17(1):27. Epub
487 2017/02/06. doi: 10.1186/s12866-017-0934-5. PubMed PMID: 28148244; PubMed Central
488 PMCID: PMCPMC5289004.
489 41. Gualdi L, Tagliabue L, Landini P. Biofilm formation-gene expression relay system in
490 *Escherichia coli*: modulation of sigmaS-dependent gene expression by the CsgD regulatory
491 protein via sigmaS protein stabilization. J Bacteriol. 2007;189(22):8034-43. Epub 2007/09/18.
492 doi: 10.1128/JB.00900-07. PubMed PMID: 17873038; PubMed Central PMCID:
493 PMCPMC2168689.
494 42. Levine JH, Lin Y, Elowitz MB. Functional roles of pulsing in genetic circuits. Science.
495 2013;342(6163):1193-200. Epub 2013/12/07. doi: 10.1126/science.1239999. PubMed PMID:
496 24311681; PubMed Central PMCID: PMCPMC4100686.
497 43. Locke JC, Young JW, Fontes M, Hernandez Jimenez MJ, Elowitz MB. Stochastic pulse
498 regulation in bacterial stress response. Science. 2011;334(6054):366-9. Epub 2011/10/08. doi:
499 10.1126/science.1208144. PubMed PMID: 21979936; PubMed Central PMCID:
500 PMCPMC4100694.
501 44. Levine JH, Fontes ME, Dworkin J, Elowitz MB. Pulsed feedback defers cellular
502 differentiation. PLoS Biol. 2012;10(1):e1001252. Epub 2012/02/04. doi:
503 10.1371/journal.pbio.1001252. PubMed PMID: 22303282; PubMed Central PMCID:
504 PMCPMC3269414.
505 45. Patange O, Schwall C, Jones M, Villava C, Griffith DA, Phillips A, et al. *Escherichia coli*
506 can survive stress by noisy growth modulation. Nat Commun. 2018;9(1):5333. Epub

2018/12/19. doi: 10.1038/s41467-018-07702-z. PubMed PMID: 30559445; PubMed Central PMCID: PMCPMC6297224.

46. Kim JM, Garcia-Alcala M, Balleza E, Cluzel P. Stochastic transcriptional pulses orchestrate flagellar biosynthesis in *Escherichia coli*. Sci Adv. 2020;6(6):eaax0947. Epub 2020/02/23. doi: 10.1126/sciadv.aax0947. PubMed PMID: 32076637; PubMed Central PMCID: PMCPMC7002133.

47. Sassi AS, Garcia-Alcala M, Kim MJ, Cluzel P, Tu Y. Filtering input fluctuations in intensity and in time underlies stochastic transcriptional pulses without feedback. Proc Natl Acad Sci U S A. 2020;117(43):26608-15. Epub 2020/10/14. doi: 10.1073/pnas.2010849117. PubMed PMID: 33046652; PubMed Central PMCID: PMCPMC7604450.

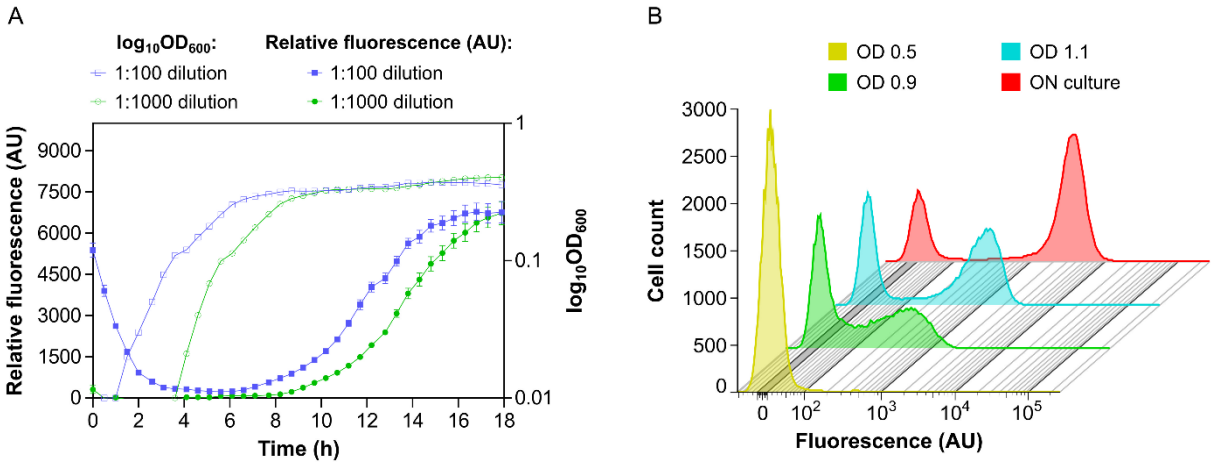

Figure 1: Bimodal activation of curli gene expression in *E. coli* planktonic cultures. *E. coli* cells carrying genomic transcriptional reporter of *csgBAC* operon were grown in liquid tryptone broth (TB) medium at 30 °C under constant shaking. **(A)** Optical density (OD_{600}) and relative fluorescence (fluorescence/OD_{600}; AU, arbitrary units) of the culture during growth in a plate reader, starting from two different dilutions of the overnight culture. Error bars indicate standard error of the mean (SEM) of 10 technical replicates. **(B)** Distribution of single-cell fluorescence levels in cultures grown to indicated OD_{600} or overnight (ON; 25 h) in an orbital shaker, measured by flow cytometry.

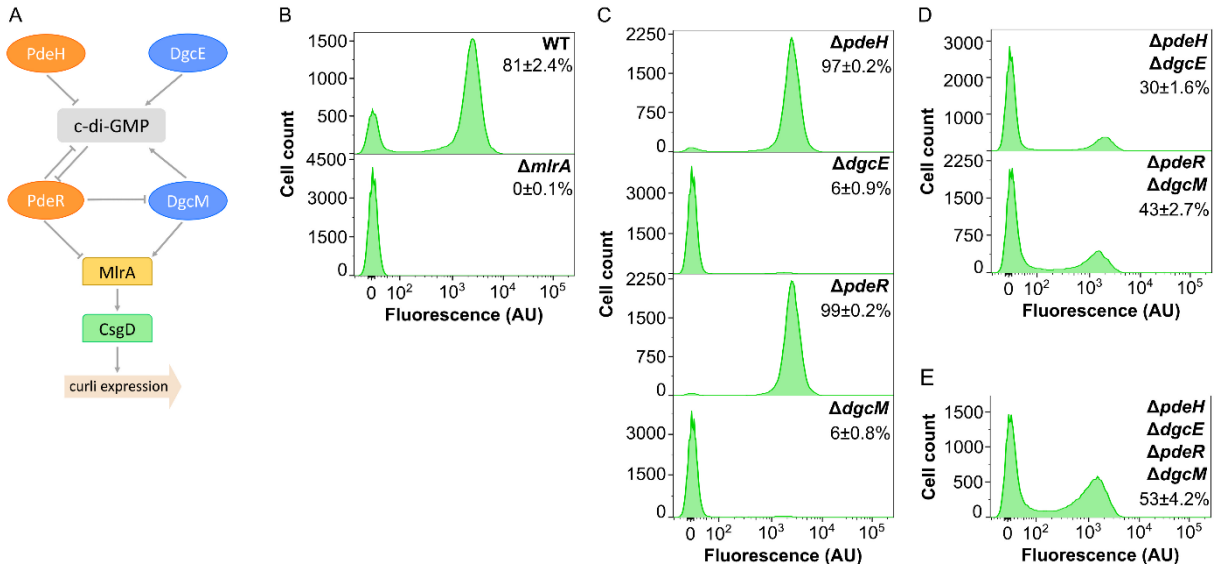

Figure 2: Regulation of curli expression by c-di-GMP. (A) Current model of regulation of curli gene expression by c-di-GMP in *E. coli*, adapted from [27]. The regulation is mediated by two pairs of diguanylate cyclases (DGCs; blue) and phosphodiestherases (PDEs; orange). PdeH and DgcE control global level of c-di-GMP, whereas PdeR and DgcM mediate local c-di-GMP-dependent regulation of curli gene expression by controlling activity of transcription factor MlrA, which activates another curli-specific transcription factor CsgD. **(B-E)** Flow cytometry measurements of curli gene expression in *E. coli* planktonic cultures grown overnight in flasks in an orbital shaker, shown for the wildtype (WT) and Δ*mlrA* knockout (B), and individual (C), double (D) and quadruple (E) knockouts of DGC or PDE enzymes, as indicated. Fraction of positive cells in the population (mean of three biological replicates ± SEM) is indicated for each strain. Note that the scale in the *y* axes is different for individual strains to improve readability.

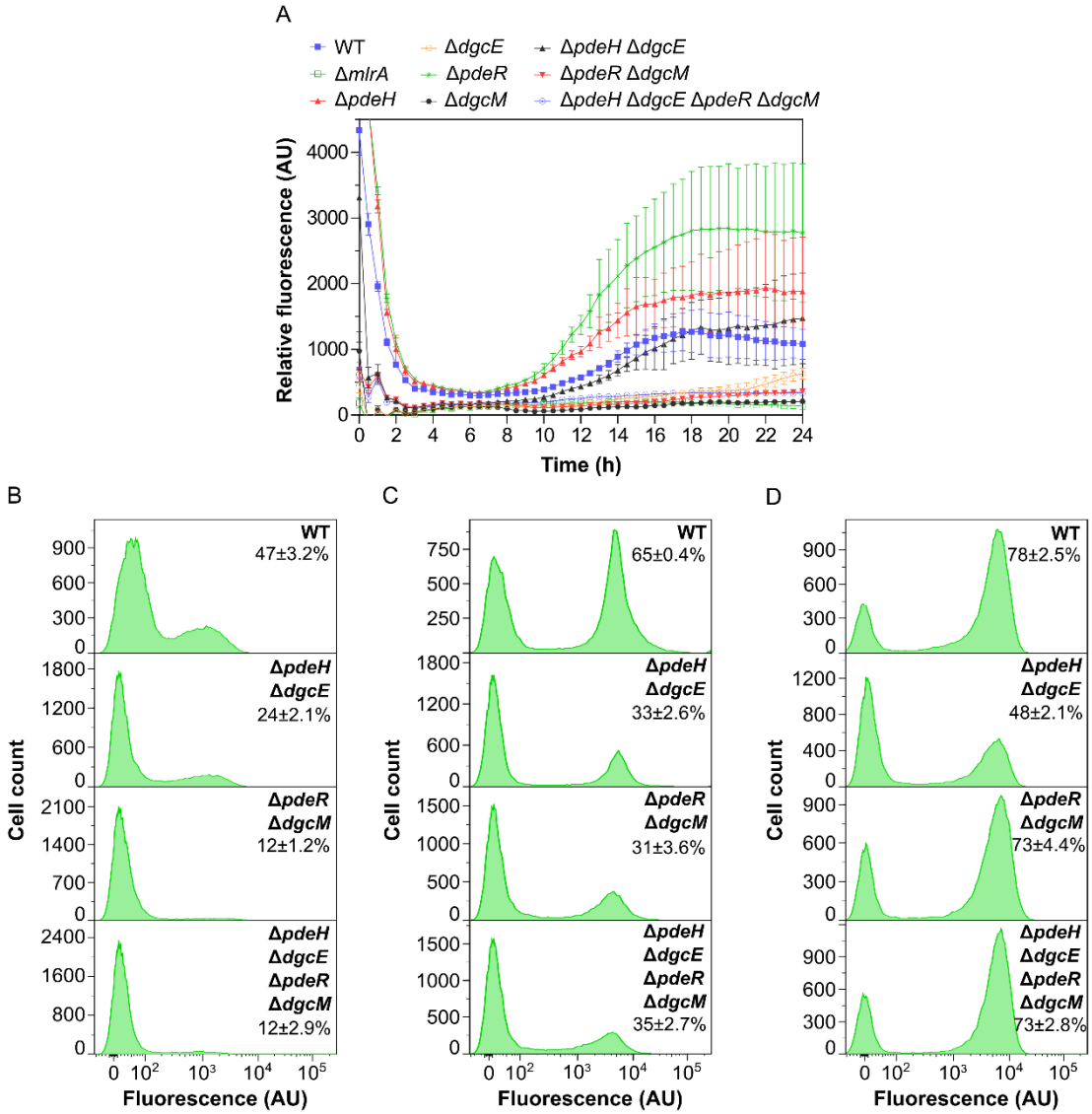

Figure 3: Dependence of curli expression on c-di-GMP regulation under different growth conditions. (A) Relative fluorescence of transcriptional curli reporter in planktonic culture grown in a plate reader. Error bars indicate SEM of 5 technical replicates. **(B-D)** Flow cytometry measurements of curli expression in the wildtype (WT) and indicated knockout strains after 24 h of growth either in a plate reader (B), as submerged biofilms (C) or as macrocolony biofilms (D). Measurements for other knock-outs are shown in Figures S4, S6A, S7A. Fraction of positive cells in the population (mean of three biological replicates ± SEM) is indicated for each strain. Note that the scale in the *y* axes is different for individual strains to improve readability.

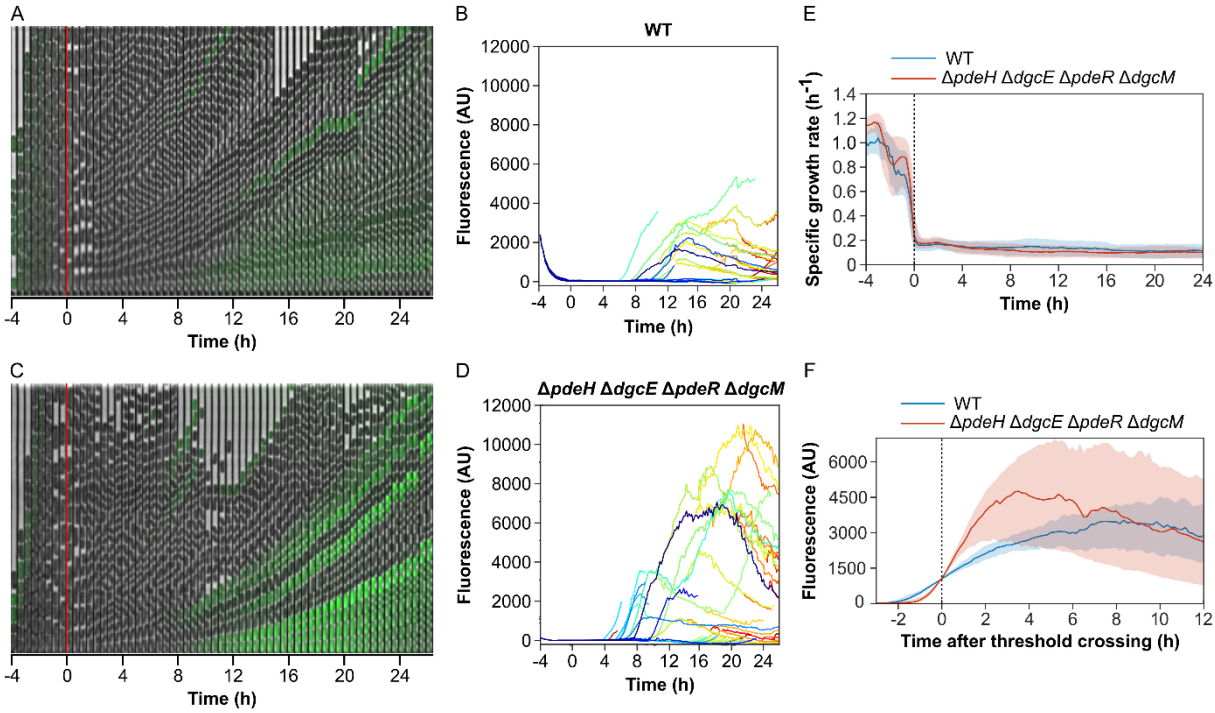

Figure 4: Impact of c-di-GMP regulation on dynamics of curli induction in individual cells. *E. coli* cells in a microfluidic device (mother machine) were shifted from a fresh to conditioned TB medium after 4 h of growth to induce curli expression. **(A-D)** Examples of image time series and single-cell fluorescence traces for the wildtype (WT) (A,B) and for the Δ*pdeH* Δ*dgcE* Δ*pdeR* Δ*dgcM* strain disabled in the c-di-GMP regulation (C,D) growing in a mother machine in one experiment. Expression of the curli reporter is indicated by the green overlay on the phase contrast image. **(E)** Median instantaneous growth rate — fold rate of change in length — of cells grown in microfluidics experiments as described in (A). The switch to conditioned medium is at time zero, as indicated. Shaded area is the interquartile range. The number of cells in the device varies with time, but is on average n = 296 for WT and n = 522 for the quadruple knockout. **(F)** Median curli expression profile for single-cell traces aligned by the time at which they exceed a threshold of 10^3 fluorescence units. Shaded area is interquartile range; n = 128 for WT and 230 for the quadruple knockout.

563 **Supporting information**

564

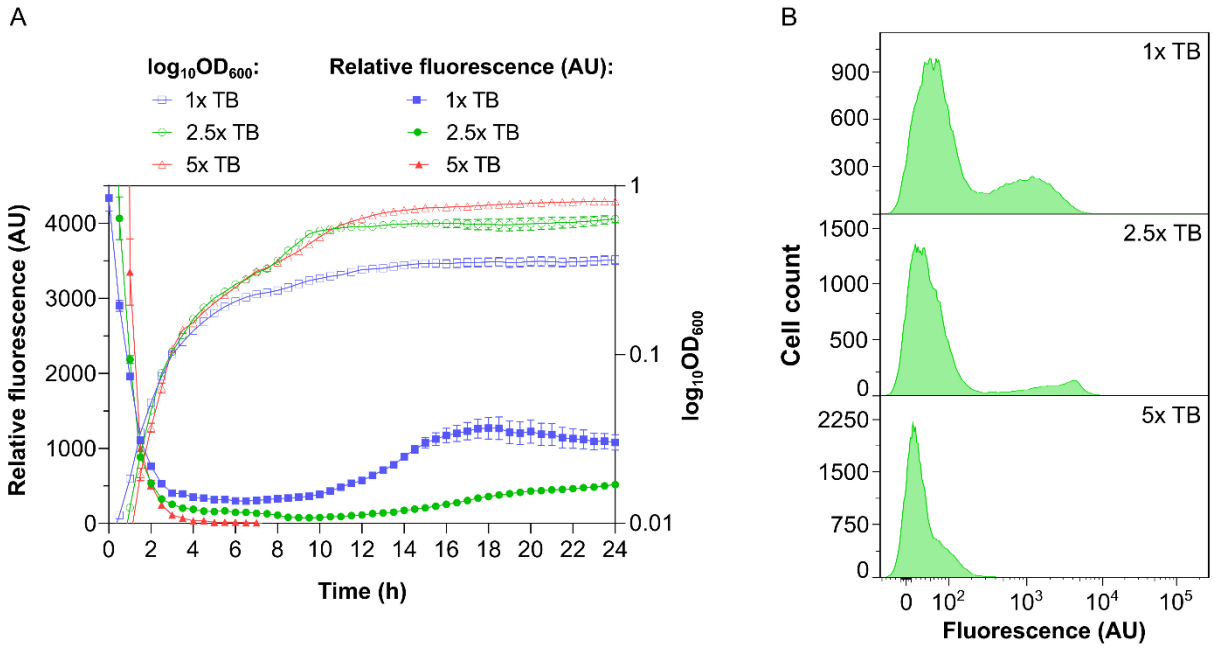

565

566 **Figure S1: Dependence of curli gene expression on nutrient levels.** Wildtype *E. coli* cultures were
567 grown as in Figure 1A but with different indicated concentrations of TB. **(A)** Bacterial growth and activity
568 of transcriptional curli reporter. Error bars indicate SEM of 6 technical replicates. **(B)** Distribution of
569 single-cell fluorescence levels after 24 h of growth in a plate reader measured by flow cytometry. Note
570 that the scale in the *y* axes is different for individual conditions to improve readability.

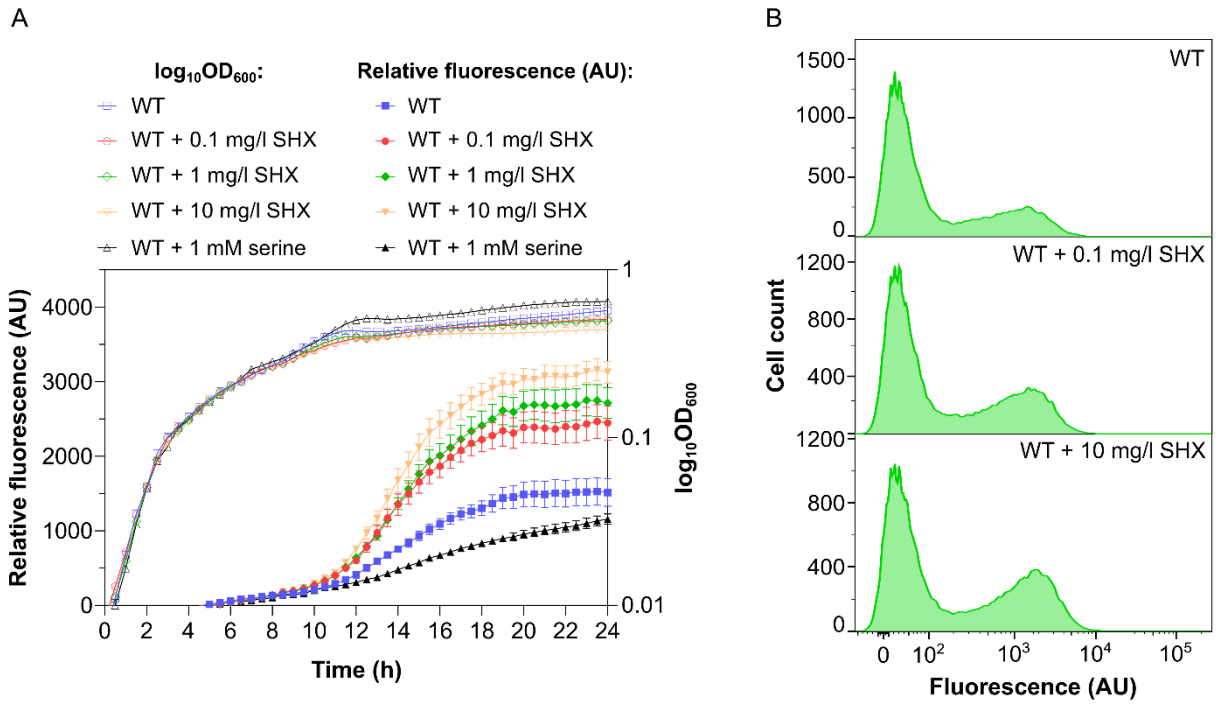

Figure S2: Stimulation of curli gene expression by stringent response. Wildtype *E. coli* cultures were grown as in Figure 1A but with addition of either indicated concentrations of serine hydroxamate (SHX) at inoculation point or 1 mM serine after 6 h of growth. **(A)** Bacterial growth and activity of transcriptional curli reporter. Error bars indicate SEM of 6 technical replicates. **(B)** Distribution of single-cell fluorescence levels after 24 h of growth in a plate reader measured by flow cytometry. Note that the scale in the *y* axes is different for individual conditions to improve readability.

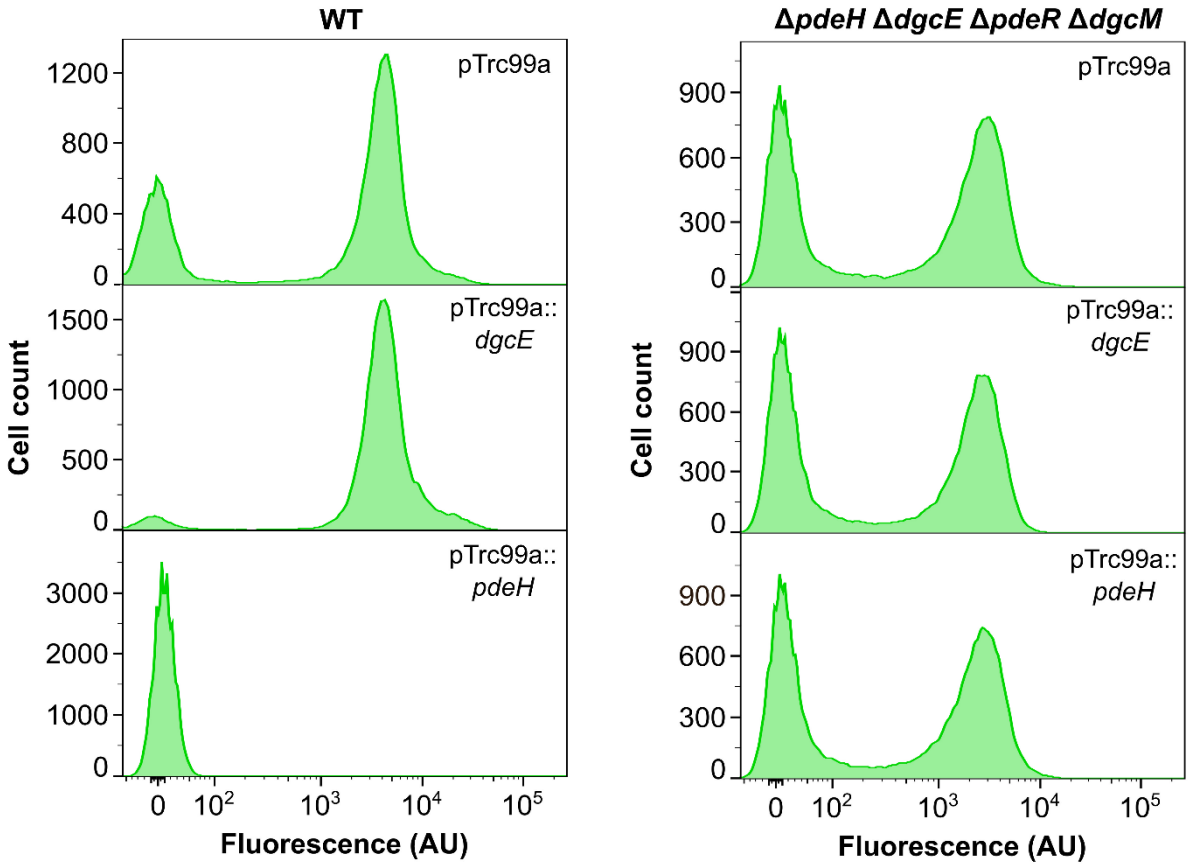

578

579 **Figure S3: Decoupling of curli gene expression from c-di-GMP regulation in the absence of PdeR/**
580 **DgcM regulatory module.** *E. coli* wildtype (WT) cells or cells lacking c-di-GMP regulatory enzymes
581 (Δ*pdeH* Δ*dgcE* Δ*pdeR* Δ*dgcM*) were transformed with either empty pTrc99a plasmid (control) or with
582 pTrc99a plasmid carrying *dgcE* (pTrc99a::dgcE) or *pdeH* (pTrc99a::pdeH) genes. Expression from the
583 vector was induced with 1 μM IPTG. Bacteria were grown overnight in flasks with shaking and cultures
584 were subjected to the flow cytometry analysis. Note that the scale in the *y* axes is different for individual
585 strains to improve readability.

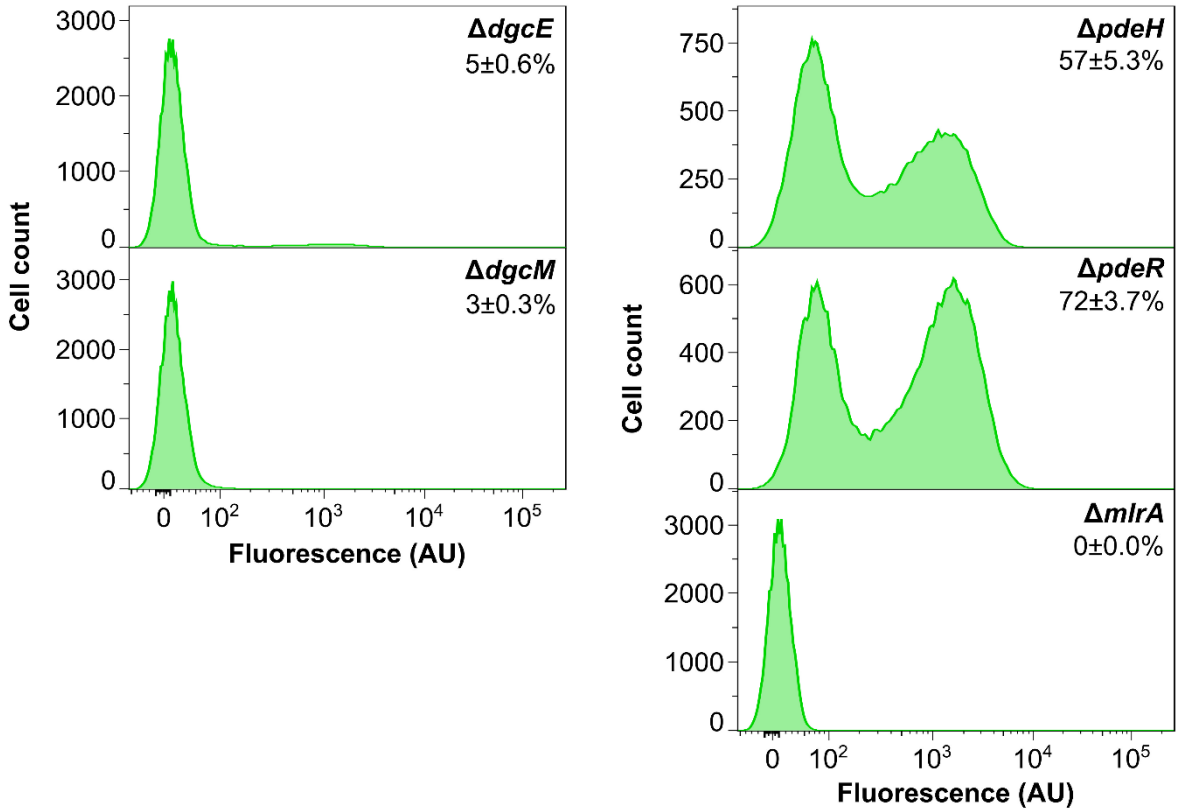

586

587 **Figure S4: Curli gene expression in cultures grown in a plate reader.** *E. coli* cells were grown as in
588 Figure 3A,B. Flow cytometry measurements for indicated knockouts are shown. Measurements in other
589 strains are shown in Figure 3B. Fraction of positive cells in the population (mean of three biological
590 replicates ± SEM) is indicated for each strain. Note that the scale in the *y* axes is different for individual
591 strains to improve readability.

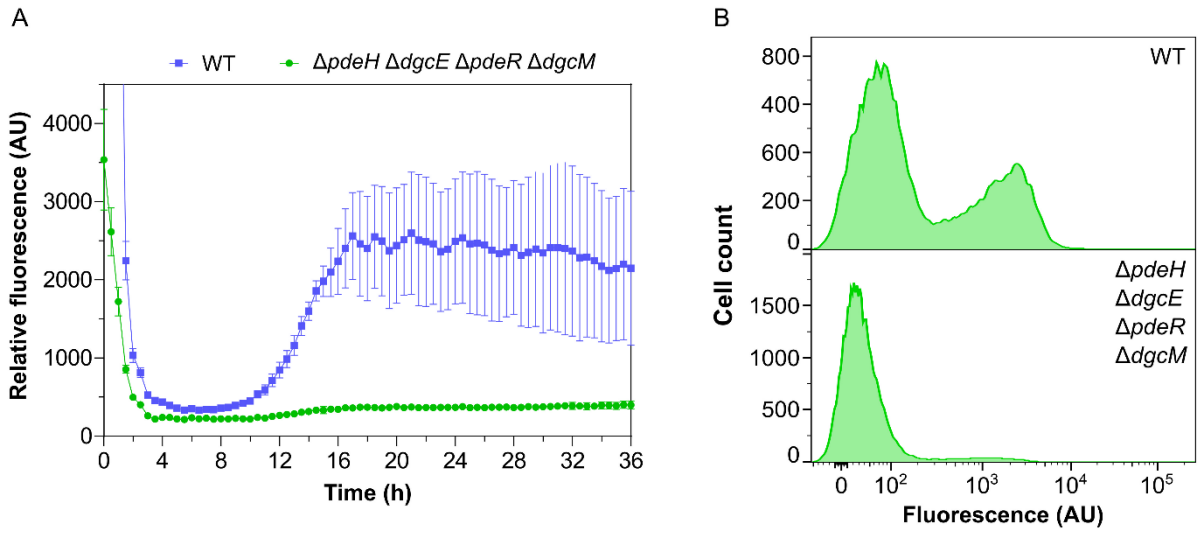

Figure S5: Curli gene expression upon prolonged cultivation in a plate reader. Wildtype (WT) and (Δ*pdeH* Δ*dgcE* Δ*pdeR* Δ*dgcM*) knockout strains were grown in a plate reader as in Figure 2 A,B, but for 36 h. **(A)** Induction of transcriptional curli reporter. Error bars indicate SEM of 10 technical replicates. **(B)** Distribution of single-cell fluorescence levels in populations of both strains after 36 h of growth measured by flow cytometry.

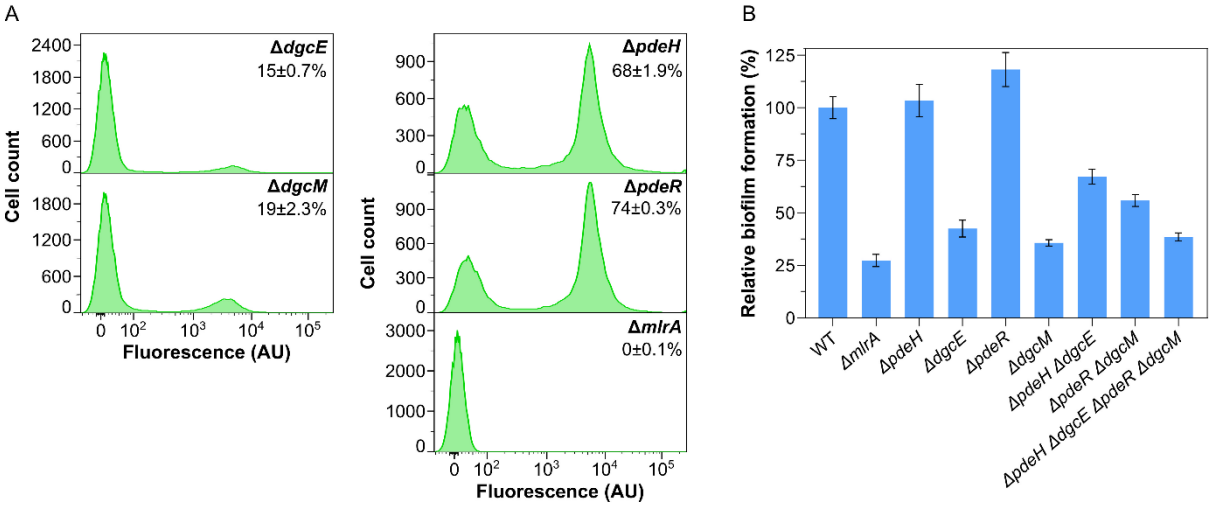

Figure S6: Curli gene expression in submerged biofilm cultures. (A) Distribution of single-cell fluorescence levels in populations of indicated knockout strains after 46 h of submerged biofilm culture growth, measured by flow cytometry. Measurements in other strains are shown in Figure 3C. Fraction of positive cells in the population (mean of three biological replicates ± SEM) is indicated for each strain. Note that the scale in the *y* axes is different for individual strains to improve readability. **(B)** Biofilm formation by indicated strains, quantified using crystal violet (CV) staining. Error bars indicate SEM of 3 independent replicates.

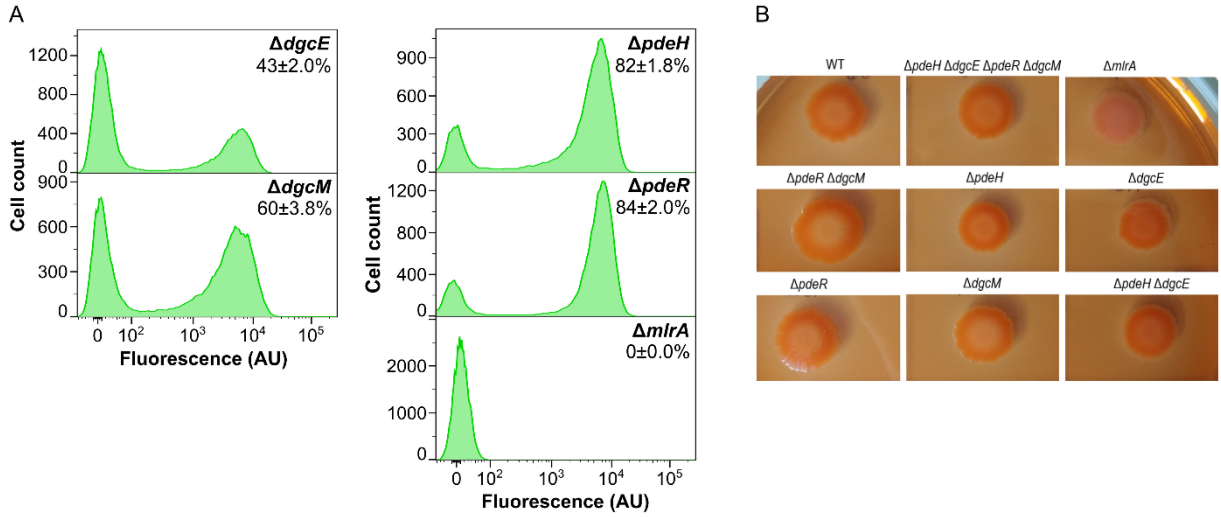

Figure S7: Curli expression in macrocolony biofilms. (A,B) Flow cytometry measurements of curli expression (A) and images of microcolonies of indicated strains (B) after 8 days of growth. Flow cytometry measurements for other strains are shown in Figure 3D. Fraction of positive cells in the population (mean of three biological replicates ± SEM) is indicated for each strain. Note that the scale in the *y* axes is different for individual strains to improve readability.

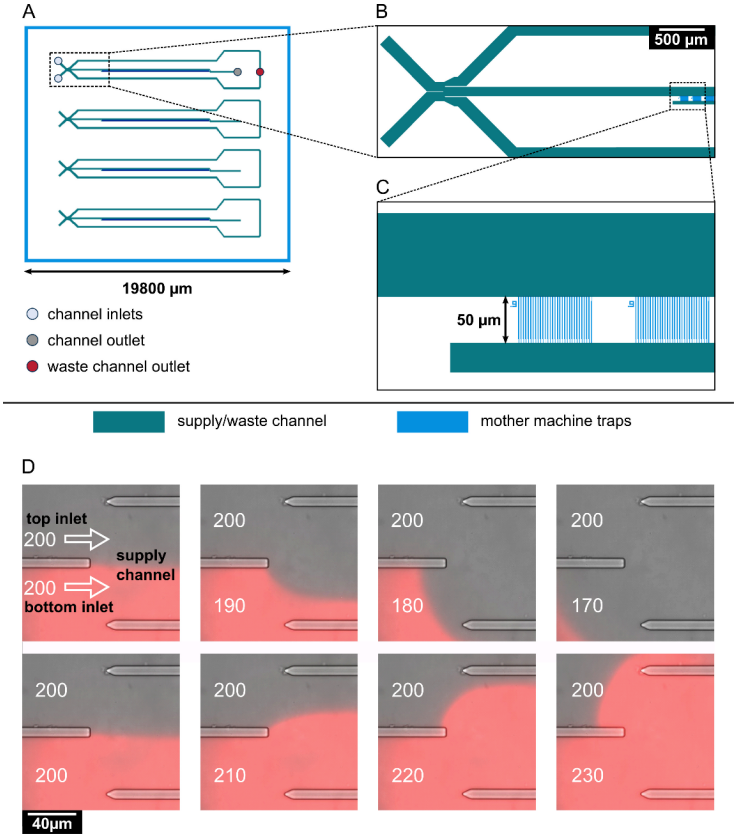

Figure S8: Design of the microfluidic mother machine chip. (A) Schematic overview on the channel layout, featuring four supply channels (green) for cell inoculation and media supply. **(B)** Detailed view of the area marked by a rectangle in (A), showing the switching junction and a part of the mother machine cultivation sites (blue). The junction is formed by two inlets, leading to one central supply channel. The control of the pressure at each inlet allows to choose the medium flowing through the supply channel, and, ultimately, to the mother machine cultivation sites. Residual medium flows out through the waste channels located on both sides from the central channel. Medium flowing through the supply channel exits the chip through one outlet. **(C)** Detailed view of the area marked in **(B)** by a rectangle, showing the mother machine cultivation sites. Each of the four channels contains 57 mother machine cultivation sites, which contain 30 mother machine traps with widths of 0.9, 1, or 1.1 µm. The mother machine traps feature a 0.3 µm wide constriction on the bottom, preventing the mother cell from exiting the trap while allowing medium perfusion. The supply channels (green) are 8 µm in depth, the mother machine traps (blue) are 0.8 µm in depth. **(D)** On-chip medium switching visualized by merged phase contrast and mCherry images of the channel junction. Media are supplied through separate inlets (top and bottom), which are separated in the center of the channel by a PDMS barrier. The direction of flow is indicated by white arrows. Water was supplied through the top inlet, while a 0.2 µM sulforhodamine B solution was supplied through the bottom inlet, visualizing the flow pattern in the junction. The pressure at the top inlet was kept constant at 200 mbar. Depending on the pressure set at the bottom inlet, it is possible to select which one of the two media flows into the central supply channel to the mother machine growth sites.

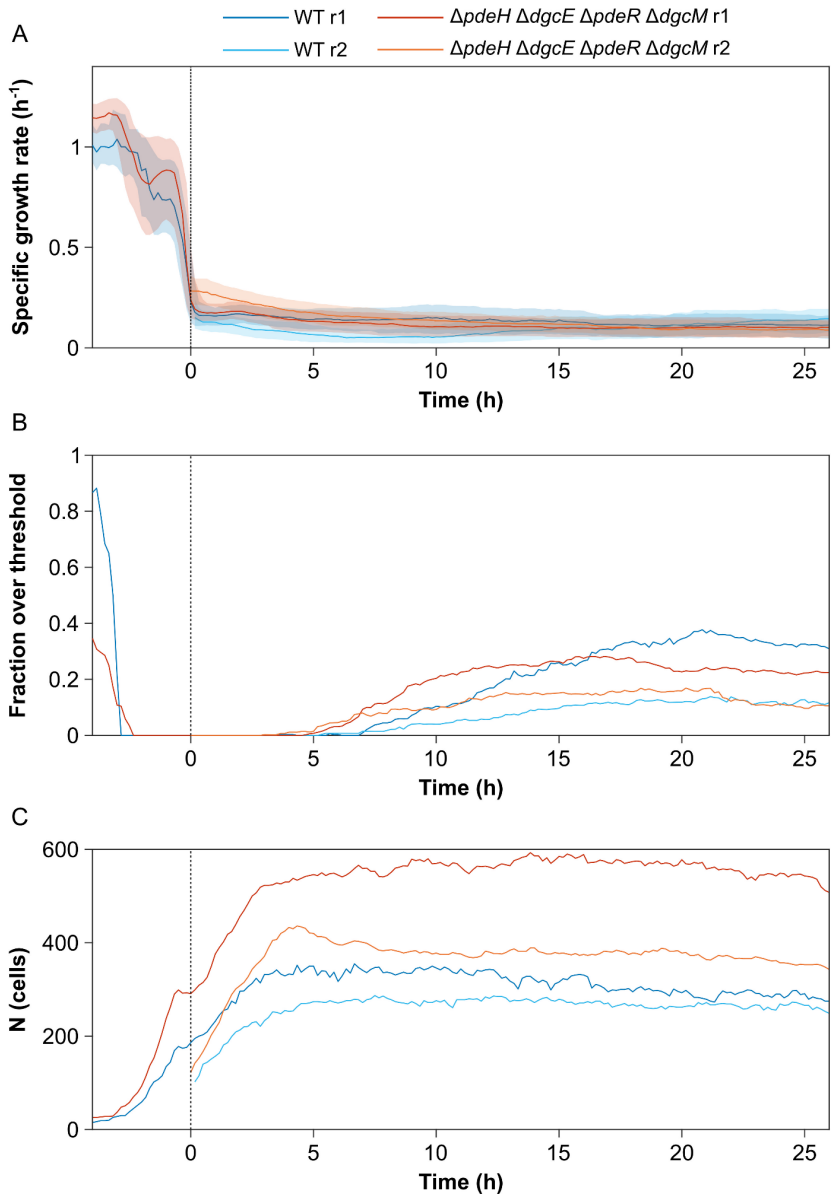

Figure S9: Growth rates and fraction of curli expressing cells over time. Stationary phase cells were introduced into mother machine devices, supplied with fresh medium and then switched to conditioned medium after four hours of growth, as in Figure 4. **(A)** Median instantaneous growth rates for the wildtype and for the Δ*pdeH* Δ*dgcE* Δ*pdeR* Δ*dgcM* strain disabled in the c-di-GMP regulation. Growth rate drops rapidly and cells switch on curli expression after a switch to conditioned medium. Shaded area is interquartile range. **(B)** Fraction of cells with fluorescence exceeding 1000 units. **(C)** Number of detected cells. Two biological replicates (r1 and r2) were performed for each strain; data for the r1 replicate are also shown in Figure 4. Note that in the experiment r2 cells were only imaged after medium switching.

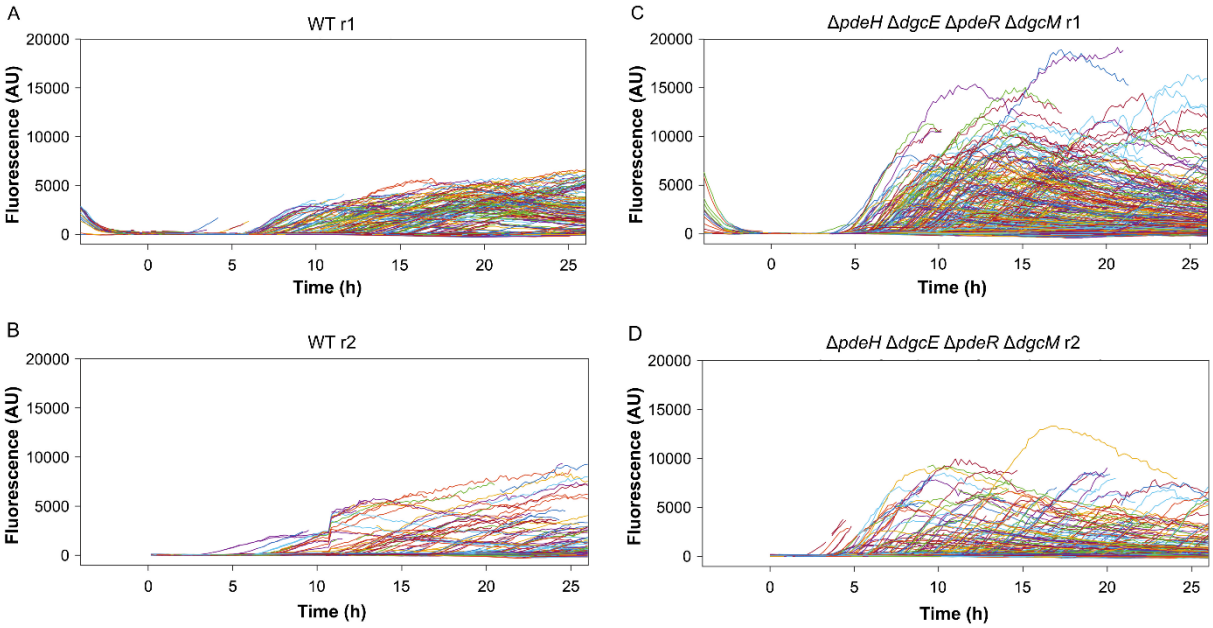

643
644 **Figure S10: Single-cell traces of cell fluorescence for all cells for the wildtype and for the c-di-**
645 **GMP-regulation disabled strain.** Data are from the same biological replicates (r1 and r2) as in Figure
646 S9.

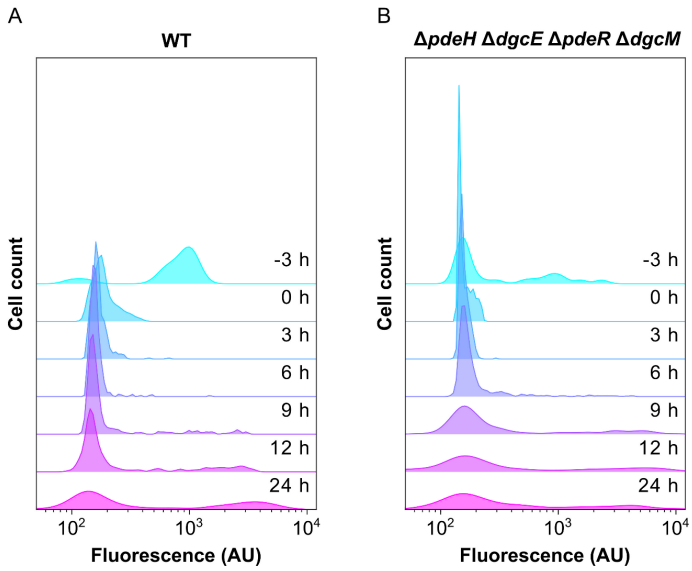

Figure S11: Distributions of curli expression at different time points in the microfluidics experiment. Shown are kernel density estimates of curli expression in the wildtype WT **(A)** and in the c-di-GMP-regulation disabled strain **(B)** at selected time points, for the replicate presented in Figure 4. In time order, for WT, n = 18, 158, 332, 317, 335, 342 and 285, and for the Δ*pdeH* Δ*dgcE* Δ*pdeR* Δ*dgcM* strain, n = 25, 247, 525, 546, 581, 546 and 544.

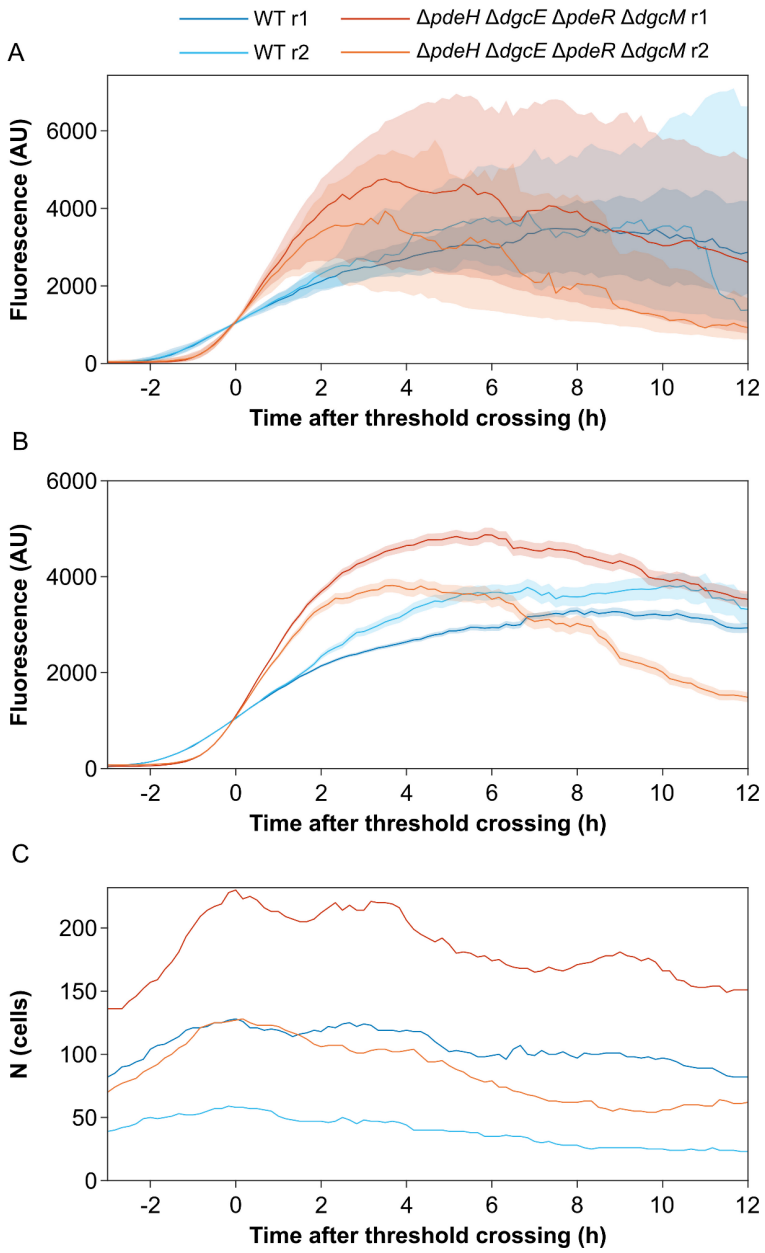

Figure S12: The rate and variability of curli induction for the wildtype and for the c-di-GMP-regulation disabled strain. (A) Median curli expression, **(B)** mean curli expression, **(C)** number of cells for traces from both microfluidics experiments (r1 and r2) aligned by the time at which they exceeded a threshold of 10^3 fluorescence units. Shaded area is interquartile range in (A) or standard error in (B). Compared to the WT, the rate of curli induction is faster but traces show more variability in a mutant without the global or local c-di-GMP regulatory modules.

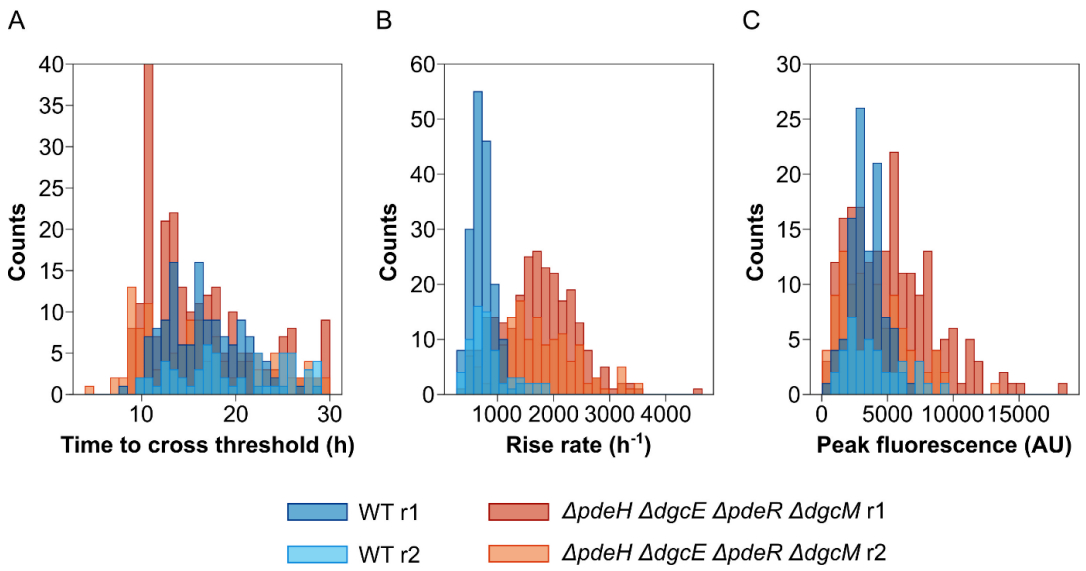

Figure S13: Distributions of curli induction parameters for the wildtype and for the c-di-GMP-regulation disabled strain. Shown are histograms of the times at which a threshold of 10^3 fluorescence units were crossed **(A)**, the maximum rates of increase in fluorescence **(B)**, or the fluorescence amplitudes at the first peak **(C)** for cell traces from both microfluidics experiments. Though switch timing is similar, rates of curli induction are faster and peak amplitudes more variable in a mutant without the global or local c-di-GMP regulatory modules.

668 **Table S1. *E. coli* strains and plasmids used in this study.**

Strains	Relevant genotype	Reference
W3110	W3110 derivative with functional RpoS	[1]
VS1146	W3110 *csgA*::*csgA*_RBS_*sfgfp*	[2]
VS1857	VS1146 Δ*mlrA*	This work
VS1732	VS1146 Δ*pdeH*	This work
VS1720	VS1146 Δ*dgcE*	This work
VS1258	VS1146 Δ*pdeR*	This work
VS1257	VS1146 Δ*dgcM*	This work
VS1717	VS1146 Δ*pdeH* Δ*dgcE*	This work
VS1713	VS1146 Δ*pdeR* Δ*dgcM*	This work
VS1729	VS1146 Δ*pdeH* Δ*dgcE* Δ*pdeR* Δ*dgcM*	This work
Plasmids		
pTrc99a	Expression vector; *Ptrc* promoter inducible by isopropyl-β-D-thiogalactopyranoside (IPTG); pBR ori; Ap^R	[3]
pVS2689	pTrc99a::*pdeH*	This work
pVS1644	pTrc99a::*dgcE*	This work

669

670 1. Serra DO, Richter AM, Klauck G, Mika F, Hengge R. Microanatomy at cellular resolution and
671 spatial order of physiological differentiation in a bacterial biofilm. mBio. 2013;4(2):e00103-13. Epub
672 2013/03/21. doi: 10.1128/mBio.00103-13. PubMed PMID: 23512962; PubMed Central PMCID:
673 PMCPMC3604763.
674 2. Besharova O, Suchanek VM, Hartmann R, Drescher K, Sourjik V. Diversification of gene
675 expression during formation of static submerged biofilms by *Escherichia coli*. Frontiers in Microbiology.
676 2016. doi: 10.3389/fmicb.2016.01568.
677 3. Amann E, Ochs B, Abel K-J. Tightly regulated tac promoter vectors useful for the expression of
678 unfused and fused proteins in *Escherichia coli*. Gene. 1988;69(2):301-15. doi:
679 https://doi.org/10.1016/0378-1119(88)90440-4.

680

681

682 **Supporting protocols**

683

684 **Design and fabrication of the mother machine.** A microfluidic device was used for time-
685 resolved studies of *E. coli* growth and curli expression, which features mother machines traps
686 for the observation of one-dimensional cell growth. The design of the microfluidic device is
687 shown in Figure S8. The channel structure of the microfluidic device features four independent
688 channels with a depth of 8 µm, allowing the realization of four conditions, e.g. different media
689 compositions, in one experiment. Each channel contains two inlets enabling on-chip switching
690 between two different media, which are supplied at defined pressures. By controlling the
691 pressure ratio between the two inlets, the medium supplied at the higher pressure flows
692 through the central channel following the junction, while the other medium is pushed away
693 from the junction and flows out through the waste channel (Figure S8D). The medium which
694 flows through the central channel reaches the mother machine cultivation sites before exiting
695 the chip through a single outlet.
696 The device was produced using a two-layer soft lithography method as described previously[1].
697 Based on our in-house made design of the channel layout, a 100 mm silicon wafer was
698 produced by e-beam lithography (ConScience, Sweden). The wafer contains the channel
699 layout as a positive relief. The mother machine traps, which are shown in blue in Figure S8A-
700 C, were structured by etching the wafer by 0.8 µm, giving the mother machine the appropriate
701 vertical dimension for cell trapping. The supply channels, which are shown in green in Figure
702 S8A-C, are implemented as photoresist structures with a height of 8 µm on the wafer. The
703 wafer served as a master mold for liquid polydimethylsiloxane (Sylgard 184 PDMS, VwR
704 International GmbH, Germany), which was mixed at volumetric ratio of 7:1 with a cross-linking
705 agent, degassed in a desiccator for 30 minutes and poured over the wafer to a height of
706 approximately 4 mm and thermally cured at 80 °C overnight. The cured PDMS was peeled off
707 from the wafer and manually cut into separate chips. Inlet and outlet holes were punched with
708 a 0.75 mm punching tool (Robbins True-Cut Disposable Biopsy Punch 0.75mm with Plunger,
709 Robbins Instruments, USA). The surface of the chip was cleaned by a rinse with isopropanol
710 and the application of adhesive tape (tesafilm, Germany) prior to bonding. The chip was
711 irreversibly bonded to a glass substrate by applying oxygen plasma to both chip and glass
712 surfaces (Diener Femto, Diener GmbH, Germany) and bringing the treated surfaces together.
713 The bond was strengthened by storing the bonded device in the oven at 80 °C for two minutes.
714 The device was mounted on an inverted fluorescence microscope (Nikon Eclipse Ti, Nikon
715 Corporation, Japan) equipped with an incubator. The microscope setup included an Andor Zyla
716 4.2 sCMOS camera (Oxford Instruments, UK), an objective with 100x magnification (Plan
717 Apochromat λ Oil, NA=1.45, WD=170 µm; Nikon, Japan) and a perfect focus system (Nikon
718 Corporation, Japan) for focus drift compensation

719

720 **Growth experiments.** *E. coli* cells were allowed to grow in TB medium until the stationary
721 phase prior to inoculation into the device. Conditioned medium was prepared by cultivating the
722 wildtype *E. coli* cells in TB medium for 20 hours, after which the cell suspension was
723 centrifuged at 4000 rpm for ten minutes, the medium was filter sterilized and stored at 4°C.
724 The mother machine growth sites were loaded with the undiluted cell suspension by manual
725 infusion of the cell suspension through one of the two inlets using a 1-ml syringe. The
726 connection between the syringe and the chip was realized by tygon tubing (Tygon S-54-HL,
727 inner diameter = 0.51 mm, outer diameter = 1.52 mm, VwR International GmbH, Germany) in
728 combination with blunt dispensing needles (General purpose tips, inner diameter = 0.41 mm,
729 outer diameter = 0.72 mm, Nordson EFD, USA). Medium flow was controlled by programmable
730 pressure regulators (LineUP FlowEZ, FLUIGENT, France), which generated flow by applying
731 pressure on 50-ml medium reservoirs (P-CAP series, FLUIGENT, France). Fresh and
732 conditioned TB medium were respectively filled in separate reservoirs, and each one was
733 pressurized by one module of the pressure regulator. After the cell inoculation both media were
734 connected to the inlets of the channel via tygon tubing and blunt dispensing needles. The
735 pressure at the inlet of the fresh TB medium was set to 200 mbar and remained constant
736 throughout the experiment. During the selection of the positions for imaging the pressure at
737 the inlet of the conditioned medium was set to 250 mbar, allowing the conditioned medium to
738 flow through the junction to the mother machine growth sites and thereby maintaining the
739 stationary state of the cells. At the beginning of imaging, the pressure at the inlet of the
740 conditioned medium was reduced to 150 mbar and programmed to increase back to 250 mbar
741 after 4 hours of on-chip cultivation, thereby activating a medium switch from fresh to
742 conditioned TB medium. Phase contrast and GFP fluorescence images were acquired with a
743 time interval of 10 min.
744

745 **Analysis of microfluidics data.** Cells were segmented from phase contrast images by
746 making use of a fully convolutional neural network based on the U-net architecture [2]. A set
747 of manually curated cell outlines was prepared for training (1105 outlines) and validation (346
748 outlines) of the network. The training set was augmented by scaling, rotation, flipping and
749 addition of white noise. A U-net of depth three, with 8, 16 and 32 filters along the contracting
750 path, was trained to predict cell interiors from phase contrast images. Phase contrast images
751 were normalized by subtracting the median and scaling to intensities expected between the
752 2nd and 98th percentiles. Cell interiors were defined from the curated outlines by filling each
753 outline and then subjecting it to two rounds of morphological erosion. The erosion step ensured
754 that neighbouring cells predicted by the network were well separated, such that distinct cell
755 instances could be clearly identified simply by thresholding the prediction and labelling

connected regions. After instance identification, two rounds of morphological dilation restored each mask to its original size. Finally, a smooth outline for each cell was obtained as a two-dimensional spline defined by equidistant knots placed on the mask edge.

To track cells between time points, we applied a length conservation strategy for the cells along each trench. At each time point, we ordered cell outlines by their depth in the trench, with deepest cells first. We then attempted to match, in order, a cell outline in time point t with one or more cell outlines in time point t+1, chosen such that the sum of their cell lengths would be conserved within some threshold tolerance. In the trivial case, the length of the first outline at time point t would match that of the first outline at time point t+1. In the event of cell division, the cell length at time point t would match the sum of the first two cell lengths at time point t+1. Since cells may grow in length between time points, we also initialised a growth rate parameter for each cell that biased the expected cell lengths for time point t+1 as a fold-increase in length. To enable adaptation to the true growth rate, the growth rate parameter was updated by a lagging average over 20 time points. To increase robustness to errors in segmentation, we additionally allowed state transitions from one to many and many to one, and built a proposal tree, which branched for all valid assignments lying within the length thresholds. We searched for the proposal with the lowest average fold-change in matched lengths, but limited branching by retaining only the 10 best proposals for subsequent nodes (cell outlines) in the tree. The length thresholds were deliberately set loosely such that the (sum of) cell length(s) at t+1 could decrease at most five-fold or increase at most two-fold relative to the (sum of) cell length(s) at t. This increased the number of valid proposals, but was important in cases where the growth rate estimate was poor. For transitions where one cell outline split into more than two, or transitions where multiple outlines merged into one cell, a new label was generated for the corresponding cells at t+1. We made one exception to this labelling strategy to account for occasional ambiguity in segmentation near division events, where a cell segmented as two sister cells could later be segmented as a single mother cell. Specifically, when two sister cells — i.e., cells that were previously involved in a division event — merged into one, the label was set back to that of the mother; at the next division event, the labels of the sister cells were also retained. Finally, note that any outlines below a minimum size threshold of 50 pixels were ignored. All errors in tracking were manually curated.

Cell length was estimated from cell regions as the ‘major axis length’ of the Matlab regionprops function — the major axis of the ellipse with same normalised second central moment as the region. Instantaneous growth rates were estimated from the derivative of a smoothing spline fitted to the logarithm of cell length over each cell division cycle. Knots for the spline were placed at intervals of at least 15 time points. Single-cell fluorescence traces were quantified from the median fluorescence within each outline. Background fluorescence varied as a function of time due to the accumulation of cells at some trench exits, so we corrected for

background fluorescence in each trench at each time point using the median value of all non-cell pixels. Fluorescence traces were characterised along branching lineages and were smoothed with a Savitzky-Golay filter of order 3 and window length 21. The derivative of the filter was used to obtain the maximum rate of fluorescence increase. In cases where multiple descendants shared a common peak event before branching, we counted that event only once.

References

1. Qin D, Xia Y, Whitesides GM. Soft lithography for micro- and nanoscale patterning. Nat Protoc. 2010;5(3):491-502. Epub 2010/03/06. doi: 10.1038/nprot.2009.234. PubMed PMID: 20203666.
2. Ronneberger O, Fischer P, Brox T. U-net: Convolutional networks for biomedical image segmentation. arXiv. 2015;[1505.04597].